



HAL
open science

The blueschist–eclogite transition in the Alpine chain: P–T paths and the role of slow-spreading extensional structures in the evolution of HP–LT mountain belts

A. Vitale Brovarone, M. Picatto, O. Beyssac, Yves Lagabrielle, D. Castellib

► To cite this version:

A. Vitale Brovarone, M. Picatto, O. Beyssac, Yves Lagabrielle, D. Castellib. The blueschist–eclogite transition in the Alpine chain: P–T paths and the role of slow-spreading extensional structures in the evolution of HP–LT mountain belts. *Tectonophysics*, 2014, 615-616, pp.96-121. 10.1016/j.tecto.2014.01.001 . hal-01947009

HAL Id: hal-01947009

<https://hal.sorbonne-universite.fr/hal-01947009>

Submitted on 6 Dec 2018

HAL is a multi-disciplinary open access archive for the deposit and dissemination of scientific research documents, whether they are published or not. The documents may come from teaching and research institutions in France or abroad, or from public or private research centers.

L'archive ouverte pluridisciplinaire **HAL**, est destinée au dépôt et à la diffusion de documents scientifiques de niveau recherche, publiés ou non, émanant des établissements d'enseignement et de recherche français ou étrangers, des laboratoires publics ou privés.

The blueschist–eclogite transition in the Alpine chain: P–T paths and the role of slow-spreading extensional structures in the evolution of HP–LT mountain belts

A. Vitale Brovarone ^{a,*}, M. Picatto ^b, O. Beyssac ^a, Y. Lagabrielle ^c, D. Castelli ^b

^a Institut de Minéralogie, de Physique des Matériaux, et de Cosmochimie (IMPMC), Sorbonne Universités - UPMC Univ Paris 06, UMR CNRS 7590, Muséum National d'Histoire Naturelle, IRD UMR 206, 4 Place Jussieu, F-75005 Paris, France

^b Dipartimento di Scienze della Terra, Università degli Studi di Torino, via Valperga Caluso 35, 10100 Torino, Italy

^c Observatoire des Sciences de l'Univers de Rennes, Géosciences Rennes - UMR 6118, 263 Avenue du General Leclerc CS 74205, 35042 RENNES CEDEX

ABSTRACT

High-pressure metamorphic rocks exhumed in mountain belts provide a unique window on deep processes at subduction zones, such as the progressive transformation of blueschist into eclogite, which has important geochemical and geophysical implications, along with information on their exhumation mechanism. We provide a detailed characterization of the field and metamorphic relationships between blueschist- and eclogite-facies terranes of Alpine Corsica (France), where both primary, pre-subduction structures and Alpine high-pressure assemblages are very well preserved. We then compare our data with available observations from the Western Alps. Altogether, these data show systematic metamorphic patterns across the blueschist–eclogite boundary: temperature increases progressively without any gap across the contact, whereas a significant pressure jump (ca. 0.4 GPa) is observed. Lithostratigraphy in the two units suggests that they belong to two different types of oceanic (or transitional) crust, structures of which may have controlled their different mechanisms of decollement, accretion and exhumation. Lastly, the comparison of the exhumed terranes in Alpine belts with structures of modern analogues in present-day oceans, such as large detachment faults and oceanic core-complexes, stresses the importance of inherited extensional structures for subduction, exhumation and orogenic processes.

Keywords:

Eclogite–blueschist transition
Lawsonite eclogite
Structural inheritance
Oceanic detachment faults in HP belts

1. Introduction

The transition from blueschist- to eclogite-facies conditions is a hot topic with profound implications in geochemistry and geophysics because of the associated dehydration and densification of oceanic subducting slabs (e.g. Hacker, 2003). The association of blueschist- and eclogite-facies rocks is widely recognized in high-pressure/ultra-high-pressure (HP/UHP) mountain belts providing a unique window on the processes occurring at depth (e.g. Brown, 2007; Maruyama et al., 1996; Ota and Kaneko, 2010; Tsujimori et al., 2006). In the internal zones of nappe-type collisional belts (e.g. review by Ota and Kaneko, 2010), these rocks form large terranes separated by decompressional tectonic discontinuities (e.g. Western Alps: Ballèvre and Merle, 1990, 1993; Corsica: Vitale Brovarone et al., 2013; New Caledonia: Vitale Brovarone and Agard, 2013), thus lacking the pristine blueschist-to-eclogite continuity.

The exhumation of blueschist- and eclogite-facies rocks requires specific conditions of decollement and accretion that are vigorously debated. Among them, the nature of the subducted plate, such as its buoyancy, the presence of major inherited structures (e.g. seamounts), may have a crucial role (e.g. Agard et al., 2009; Cloos, 1993; Ernst et al., 1997). In addition,

in many HP belts where remnants of oceanic subducted units are preserved, such as the Alps (Western Alps, Corsica), the transition from blueschist- to eclogite-terrane remarkably matches a lithological contrast. Metasedimentary rocks dominate the blueschist units and metaophiolites dominate the eclogite units. The interpretation of this lithological and metamorphic contrast is twofold. Some authors interpret this contrast as the consequence of the progressive offscraping of oceanic sedimentary cover rocks at the base of a “shallow” blueschist-facies accretionary prism, and the subsequent eclogitization of the “bypassed” oceanic basement at greater depths (Agard et al., 2009 and references therein; Marthaler and Stampfli, 1989). Other authors, focusing on the lithostratigraphy of these two terranes and their equivalents in present day slow-spreading oceans, suggest that they originated in two different types of oceanic settings, magma-poor and magma-rich, respectively (e.g. Lagabrielle and Lemoine, 1997), the structures of which favor different types of decollement and accretion during subduction (see discussion in Tricart and Schwartz, 2006).

The aim of this contribution is to clarify the nature of the metamorphic and lithological patterns across the blueschist–eclogite contact zone in Alpine HP mountain belts by means of (i) a detailed tectonostratigraphic characterization of the blueschist–eclogite transition in the Schistes Lustrés complex, together with (ii) new, high-spatial resolution petrological data obtained by means of Raman

* Corresponding author.

E-mail address: alberto.vitale-brovarone@impmc.upmc.fr (A. Vitale Brovarone).

spectroscopy of carbonaceous material (RSCM) thermometry and P–T pseudosection. We selected Alpine Corsica as a case study because late deformation is localized, and both primary oceanic structures and HP–LT assemblages are extremely well preserved and crop out over an accessible area. The tectonostratigraphic and metamorphic observations and data from Corsica are then compared with the extensive lithostratigraphic and metamorphic literature available for the Western Alps. Petrological estimates across the blueschist–eclogite boundary show characteristic patterns in the two belts. We discuss the nature and implication of these patterns in the final part of the paper, together with a reinterpretation of the role of the oceanic structural inheritance on the Alpine orogenesis based on the latest research developments about slow-spreading oceanic structures.

2. Geology of the Schistes Lustrés of Corsica and comparison with the Western Alps

Alpine Corsica represents a unique example of Alpine orogenic belt where both pristine oceanic structures and HP–LT mineral assemblages, especially lawsonite–eclogite are well preserved (Lahondère, 1996; Ravna et al., 2010; Vitale Brovarone et al., 2011a,b). This belt originated from the closure of the slow-spreading Tethys Ocean, and shares lithostratigraphic and tectonometamorphic similarities with the Western Alps (e.g. Audaudric du Chaffaut, 1972; Lagabrielle and Lemoine, 1997; Lemoine, 2003). However, some debate exists on whether or not the two belts derive from the same subduction or from two distinct and opposite subduction zones (see e.g. Molli, 2008; Principi and Treves, 1984; Vitale Brovarone and Herwartz, 2013).

Alpine Corsica occupies the northeastern part of the island of Corsica, and overthrusts the mostly granitic Hercynian Corsica, to the west (Fig. 1A, B). Three main domains are recognized in Alpine Corsica (Durand-Delga, 1978; Jolivet et al., 1990; Malavieille et al., 1998; Mattauer et al., 1981; Molli et al., 2006; Vitale Brovarone et al., 2013): (i) the Corsica continental margin units, which experienced low-grade blueschist conditions during the Alpine orogeny, (ii) the Schistes Lustrés complex, named by the French authors after its equivalent in the Piemonte Zone in the Western Alps, and showing low-grade to eclogite-facies HP/LT conditions, and (iii) the low-grade “Nappes Supérieures”, including weakly metamorphic ophiolites (e.g. Balagne–Nebbio–Pineto–Inzecca), equivalent to the Chenaillet unit in the Western Alps, and pieces of continental basement (e.g. Caporalino–Pedani, Santa Lucia, Fig. 1A) (average subgreenschist-facies metamorphic conditions, ca. 300 °C/0.3 GPa).

The internal geology of the Schistes Lustrés complex includes several tectonometamorphic units forming altogether a large antiformal structure (cf. review by Vitale Brovarone et al., 2013 for details). As in the Western Alps, within the Schistes Lustrés complex the Alpine HP/LT metamorphism increases downward, from low-grade blueschist to lawsonite–eclogite-facies conditions. The only exception in Alpine Corsica is the Castagniccia unit, which underlies the highest-grade eclogite unit and shows slightly lower, blueschist-to-eclogite-facies metamorphism. However, the paleogeographic meaning of this unit and its geodynamic significance are probably distinct from the ophiolitic units of the Schistes Lustrés considered in this work (see Discussion). We herein focus on three of the HP ophiolitic units that correspond to the transition from blueschist- to eclogite-facies conditions in ocean(s.l.)-derived units, namely the *Low-grade blueschist Inzecca unit*, the *Lawsonite–blueschist unit* and the *Lawsonite–eclogite unit*. The two first units were merged in one single in this study (see below and Fig. 1B). The main tectonostratigraphic and metamorphic features of these units are summarized as follows.

1. The *Low-grade Inzecca blueschist unit* consists of Tethyan-type metaophiolites and their Jurassic–Cretaceous metasedimentary cover rocks, the so-called Inzecca Formation (Audaudric du Chaffaut, 1972; Lagabrielle and Lemoine, 1997). A characteristic feature of

this unit, also known as the Erbajolo Formation (Early Cretaceous, Caron and Delcey, 1979), is the occurrence of metamorphosed mafic (especially gabbro) and ultramafic bodies included within a pelite-rich metasedimentary matrix. Analogues of this unit occur in the Queyras–Ubaye zone of the Western Alps (e.g. Replatte Formation) and in the low-grade metamorphic units of the Northern Apennines (e.g. Casanova mélange) (Lemoine, 2003 for review). They are regarded as remnants of both extensional and compressional gravitational deposits on the basis of comparison with similar deposits in modern oceans (Lagabrielle and Cannat, 1990; Lagabrielle and Lemoine, 1997). Metamorphic conditions are estimated at ~350 °C and 0.6–1.0 GPa (Levi et al., 2007; Vitale Brovarone et al., 2013; cf. petrological results in this study for new P estimates).

2. The *Lawsonite–blueschist unit* shows a similar lithological assemblage compared to the *Low-grade blueschist unit*, especially to the Inzecca/Erbajolo metasedimentary formation (cf. Vitale Brovarone et al., 2013 and ref therein). However, it locally includes continent-derived material such as detrital intervals within metasedimentary sequences, the so-called “Santo Pietro di Tenda unit” (Caron and Delcey, 1979), and slices of basement rocks that are ascribed to a Tethyan Ocean–Continent Transition (OCT) zone (Meresse et al., 2012; Vitale Brovarone et al., 2011b). The occurrence of continental-basement debris within blueschist-facies metasedimentary rocks of this unit is an additional point of comparison with the Schistes Lustrés of the Western Alps, where comparable associations are found (e.g. Rocher Blanc breccias, Caby et al., 1971; Lago Nero Formation, Polino and Lemoine, 1984). Metamorphic conditions are slightly higher compared to the low-grade blueschist unit and are estimated at ~450 °C and 0.8–1.0 GPa (Vitale Brovarone et al., 2013). New petrological data provide higher pressure estimates (this study, see below); the HP metamorphism is dated at ~37 Ma by means of Lu–Hf on lawsonite (Vitale Brovarone and Herwartz, 2013).

3. The *Lawsonite–eclogite unit* significantly differs from the previous units. It is rich in metaophiolites, most notably serpentinites and metabasalt, and associated metasedimentary rocks belonging to the calcschist-rich Castagniccia Formation (Caron and Delcey, 1979). Metagabbro-rich zones mostly occurs in the northern part of the unit (Cap Corse). These remnants are interpreted to represent a magmatic segment of the Tethys basin, and show lithostratigraphic characters very similar to those of the eclogite-facies units exposed in the Piemonte Zone of the Western Alps (e.g. Monviso/Rocciavré/Zermatt–Saas area, Lagabrielle and Lemoine, 1997; Lombardo et al., 2002). Based on tectono-stratigraphic considerations, in particular the occurrence of slivers of continental-basement rocks primarily associated with ultramafics, this unit has been ascribed to a distal continental margin (Lahondère, 1996) or more recently to an OCT zone (Vitale Brovarone et al., 2011b). Similar associations are found in the eclogite-facies units of the Western Alps, where Mesozoic continental extensional allochthons are described (Beltrando et al., 2010a). Metamorphic conditions are estimated at ~490–550 °C and 1.9–2.4 GPa (Ravna et al., 2010; Vitale Brovarone et al., 2011a,b), and most recent radiometric estimates point to a Late Eocene metamorphic climax (~34 Ma) by means of U–Pb on zircon (Martin et al., 2011) and Lu–Hf on garnet (Vitale Brovarone and Herwartz, 2013).

3. Tectonostratigraphy

The study area is located south of the Golo Valley and comprises the three units of the Schistes Lustrés described above, together with low-grade material of the Nappes Supérieures including both ophiolites and continental basement rocks of the so-called Caporalino–Pedani unit (Puccinelli et al., 2012) (Fig. 1B). Previous studies in the same area refer to the three above-mentioned units with local names, such as Lento–Caseluna unit for the low-grade blueschist Inzecca unit, Campitello–Morosaglia unit for the lawsonite–blueschist unit and Volpajola–San Petrone unit for the lawsonite–eclogite unit (Lahondère, 1996; Levi

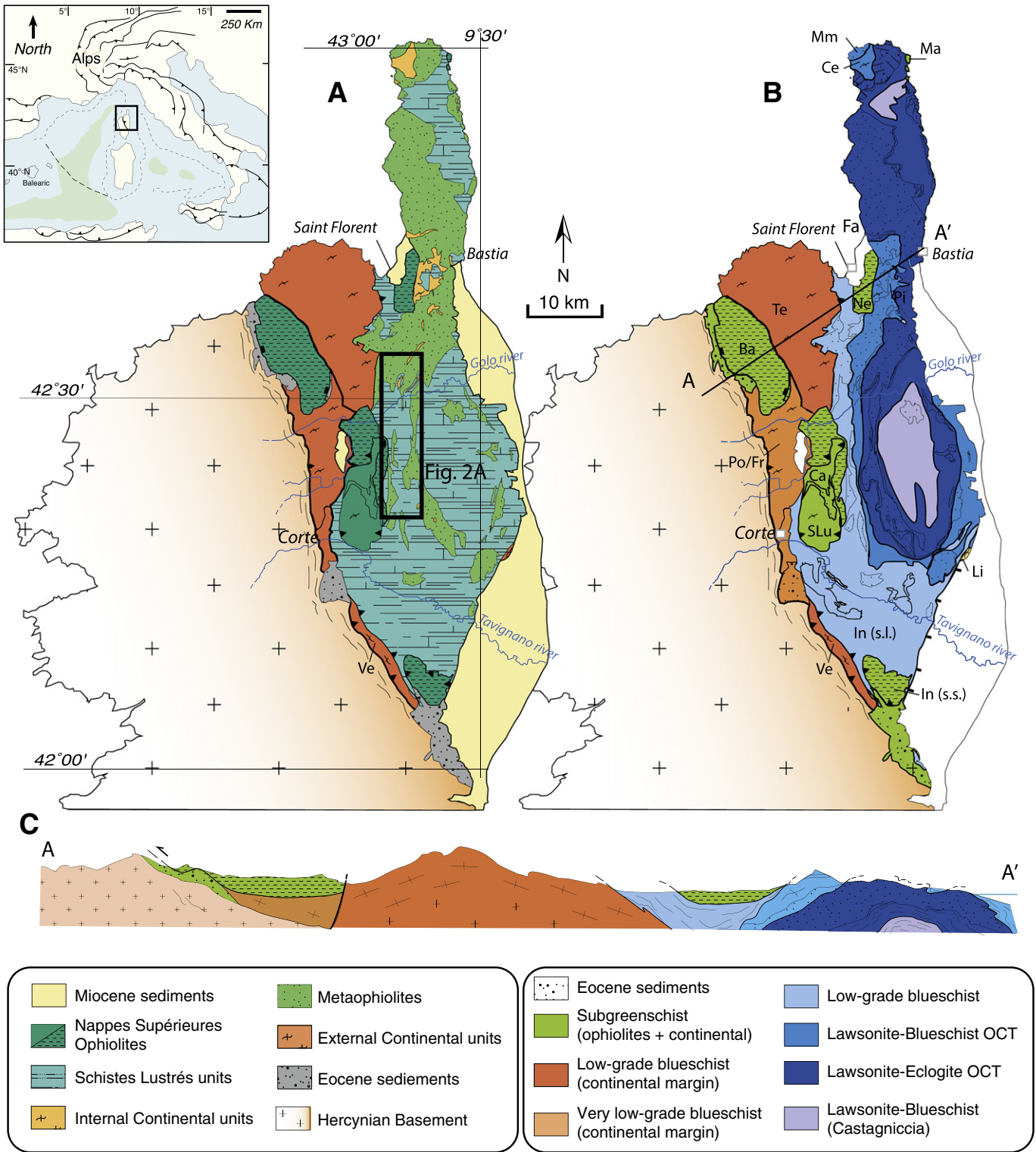


Fig. 1. A) Simplified geological map of Alpine Corsica. B) Metamorphic map of Alpine Corsica. C) Interpretive geological cross-section of Alpine Corsica (localization on Fig. 1B). Modified after Vitale Brovarone et al., 2013.

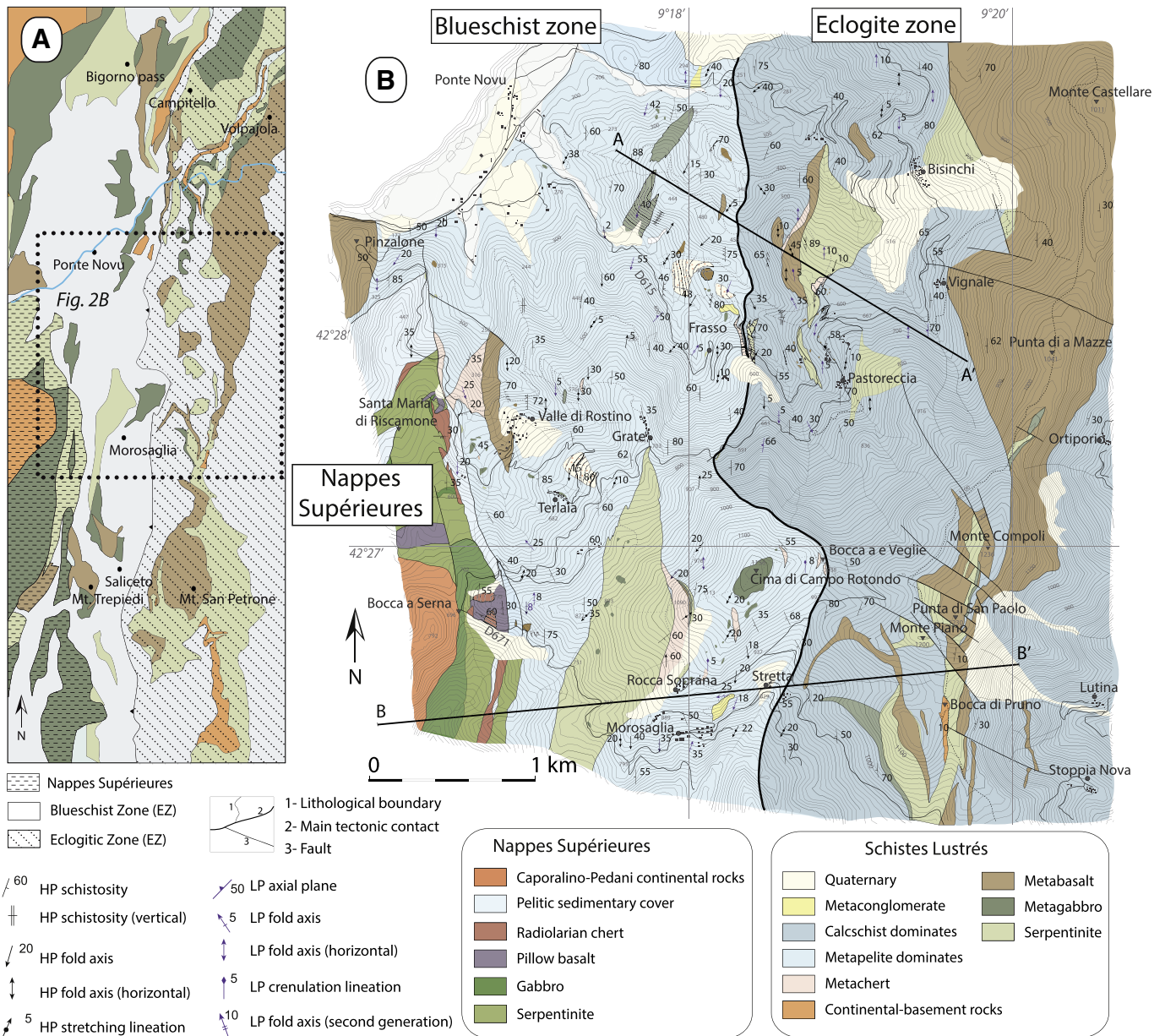
et al., 2007; Péquignot and Potdevin, 1984; Rossi et al., 2002; Vitale Brovarone et al., 2013).

Rocks from the Nappes Supérieures are beyond the scope of this paper, and we focus herein on the HP/LT units of the Schistes Lustrés. Based on the result of this study, the three above mentioned units of the Schistes Lustrés were grouped into two main zones, a blueschist-facies, metasediment-rich zone to the west (blueschist zone – BSZ hereafter), and an eclogite-facies, metaophiolite-rich zone, to the east

(eclogite zone – EZ hereafter) (Fig. 2). The BSZ comprises both the *Low-grade blueschist unit* and the *Lawsonite blueschist unit*, and the EZ corresponds to the *Lawsonite eclogite unit*.

3.1. Blueschist zone (BSZ)

Metaophiolites comprise serpentinites, ophicarbonates, metagabbros and minor metabasalts. They include: (i) rather pristine remnants of



ophiolitic basement overlain by sedimentary cover rocks, (ii) ophiolite metabreccias intercalated within metasedimentary sequences, and (iii) isolated mafic/ultramafic blocks in a metasedimentary matrix.

i. One large body of serpentinized basement and associated mafic and sedimentary cover rocks crops out in between the village of Grate and the Trepiedi mount (Fig. 2A, B). Serpentinities form a ca. 5 km long body, and consists of undeformed, variably serpentinized peridotites or intensely sheared serpentinites. Relicts of the primary pyroxene are commonly found to the west of the village of Morosaglia (Fig. 2). Ultramafics may contain gabbroic intrusions either as remnants of large magma bodies or as small dykes. Both Fe–Ti- and Mg–Al-rich metagabbros are found, but the latter are more abundant. They are characterized by a strong grain-size variation and exhibit relicts of primary phases, such as clinopyroxene and locally brown hornblende, the latter being typical of oceanic

metamorphism in Tethyan gabbros (e.g. Caby, 1995). The gabbroic dykes occur within serpentinites and are generally weakly deformed. Large metagabbro bodies are in some cases directly capped by metasedimentary rocks. In such cases, metagabbros exhibit a more intense deformation than metagabbros included in serpentinites, which may have originated during either oceanic processes or subduction, or a superposition of both stages (see Discussion). Possible primary relationships can be observed in the Morosaglia area, where a large metagabbro body is overlain by phyllite-bearing quartzites, followed upwards by metapelites and marble layers. This composite mafic/ultramafic basement is variably overlain by ophicarbonates, ophiolite breccias or metasedimentary rocks. Ophicarbonates capping serpentinized peridotites are best exposed in the northern part of the studied area, at the Bigorno pass (Figs. 2A, 4A), where they likely correspond to carbonated peridotites/serpentinities (Klein and Garrido, 2011) comparable to

those recently described in the Totalp area of the Central Alps (Picazo et al., 2011). Metabasalts are rare, and mostly occur in two isolated spots in the northeastern part of the study area (Pinzalone, Fig. 2B) and, to the south, in the Saliceto–Trepiedi basaltic massif (Fig. 2A). They consist of both pillowed flows and basaltic breccias. In the Pinzalone–Santa Reparata area, a large body of dominant pillow basalts overlies serpentinites. In the Saliceto–Trepiedi area, a ca. 200 m thick pillow basalt pile caps serpentinites and associated metagabbros. Several mafic bodies classified as metabasalt in the official geological cartography of this area (BRGM, 1:50,000, Rossi et al., 1994, 2002) commonly contain variably deformed ophiolitic breccias mostly consisting of gabbro or microgabbro clasts, and more rarely pillow breccia (see below).

- ii. Ophiolite metabreccias are found at various levels within the metasedimentary sequence, and variably consist of mafic, ultramafic and ophicarbonates. Locally, they represent the basal metasedimentary rock, lying atop of mafic/ultramafic basement rocks. Their detrital origin is often masked by the Alpine deformation, but undeformed volumes commonly preserve the pristine textures. Outcrops at the Bigorno pass best show preserved polygenic metabreccias comprising angular or rounded clasts of gabbro, microgabbro and ophicarbonate (Fig. 3A, B, C). This metabreccia corresponds to the “Trondhjemite unit” of Rossi et al. (2002), and widely occurs in the low-grade blueschist unit across the Golo Valley. Several horizons of metabreccia are found within metapelites, ranging in thickness and length from a few tens of centimeters to several tens of meters. Locally, they show a mixed mafic/ultramafic composition, or they consist mainly of large fragmented magmatic pyroxene crystals (e.g. close to the Terlaia Church, Fig. 2). In other cases, thin (5–20 cm thick) chlorite–ankerite–fuchsite-rich layers intercalated within metapelites likely correspond to former mafic/ultramafic detrital horizons (Fig. 3D). More locally, ophiolite metabreccias mostly consist of basaltic clasts (Fig. 3E).
- iii. Isolated blocks of serpentinite or metagabbro are also found within the metasedimentary sequence throughout the BSZ. Blocks of metagabbro locally contain basaltic meta-dykes (Fig. 3F), which indicate their pristine igneous structure. Spectacular examples are exposed in the area of Rocca Soprana, where blueschist-facies metagabbro cut by metabasaltic dykes also preserve primary chilled margins now overgrown by blueschist-facies mineral assemblages.

Metasedimentary rocks form a ~2300 m thick sequence mostly comprising metacherts, metapelitic schists, marbles and, locally, metaconglomerates. Metacherts occur as both the lowest structural term of the oceanic cover of the ophiolitic basement and as thick layers or isolated blocks within the metapelite sequence. They mostly consist of quartz and phyllosilicates; no Mn-rich phases, such as garnet or piemontite, were found.

Metapelites are the most abundant metasedimentary rock type of the BSZ, and consist of thin alternations of fine-grained lepidoblastic layers, mostly consisting of phengite/paragonite and chlorite, and granoblastic quartz and/or carbonate (likely calcite after aragonite) layers. In the western part of BSZ, metapelites are richer in carbonate compared to the eastern part (Fig. 4A). Metapelites commonly contain albite and/or HP Na-rich phases, such as glaucophane, and are rich in chlorite. This Fe–Mg enrichment possibly indicates reworking of fine-grained magic/ultramafic material or a volcano-sedimentary/tuffitic protolith.

Marbles form layers from a few cm to ~1 m thick, variably intercalated within the metapelites. They are light gray on the weathered cut, and

dark gray on the fresh one. On the weathered cut, they commonly show small darker dots consisting of dusty carbonate crystals in thin section. These layers possibly correspond to partially recrystallized metacalciturbidites. Chlorite-rich marbles are locally found in contact with serpentinites. They are characterized by dark, chlorite-rich thin layers and by reddish carbonate clasts. This particular lithology likely represents carbonated serpentinites (see above).

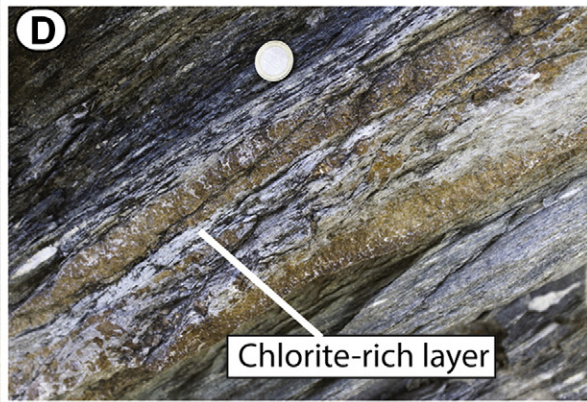
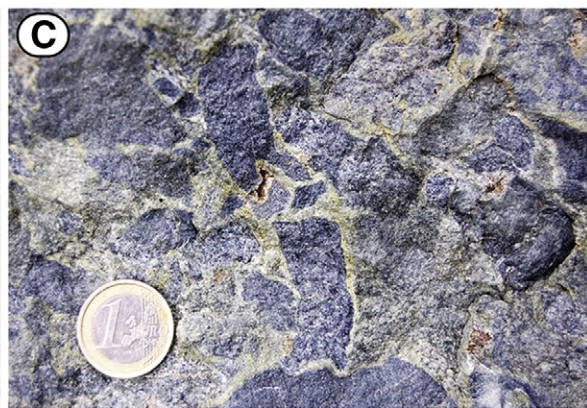
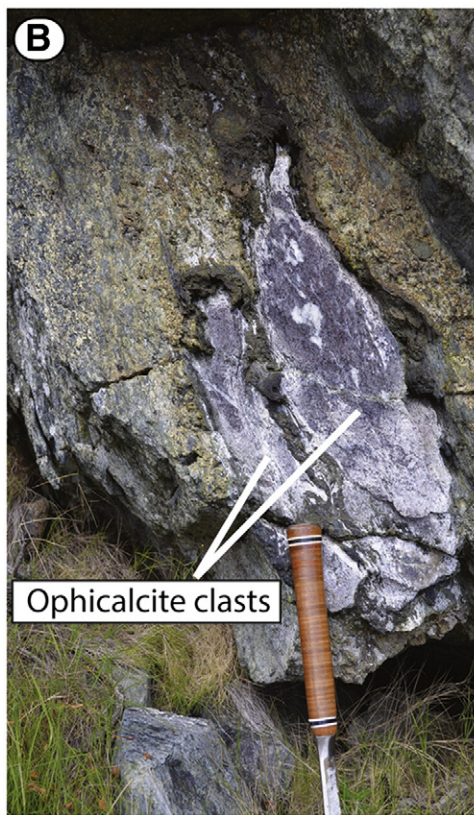
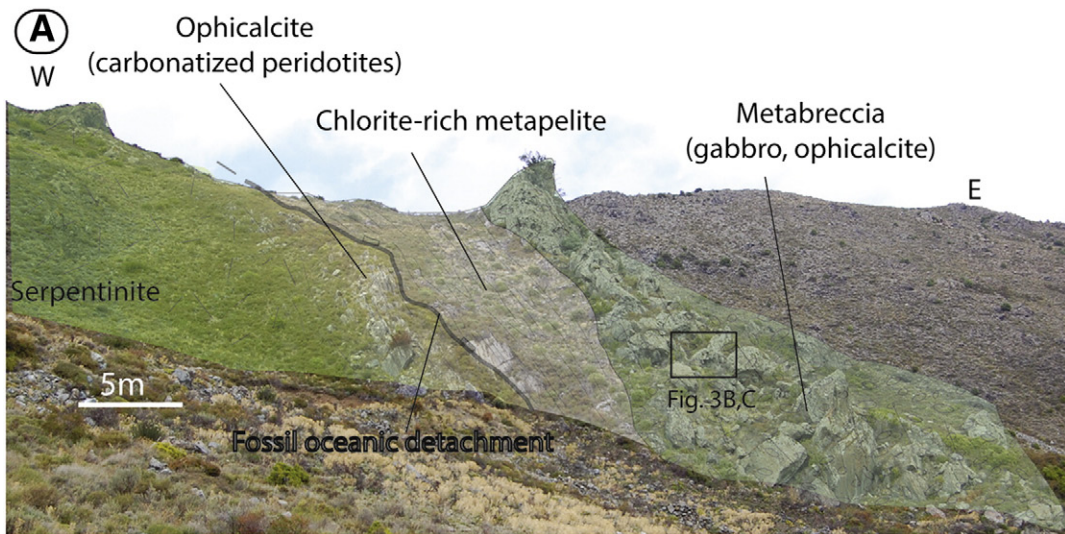
Continent-derived *metaconglomerates* are observed in three main lenses outcropping close to the contact with the EZ. Two of them were already reported in the literature to the west of Bisinchi (Rossi et al., 2002) and below the Santa Reparata church in Morosaglia (Fig. 4C; Vitale Brovarone et al., 2011b) whereas we found the third slice in the area of Castello di Rostino. These conglomerates mostly consist of acidic clasts of plutonic and volcanic origin. However, different facies characterize the Morosaglia and Castello di Rostino lenses. The former mostly comprises meta-acidic clasts and minor carbonate and mafic clasts dispersed in an arkosic matrix (Fig. 4B, C, D, E, F). Acidic clasts range in size from a few centimeters to about one meter, and are poorly deformed. Carbonate clasts are typically stretched and form elongated lenses (Fig. 4F). Mafic clasts (Fig. 4E, F) are fine-grained and sulfide-rich, and their texture in thin section mismatches with typical ophiolitic basalts. The Castello di Rostino lens contains both acidic (Fig. 4G, H) and gabbroic (Fig. 4I) clasts of variable size, from cm-size (Fig. 4G) to large boulders (Fig. 4H), dispersed in a metapelitic matrix (Fig. 4G, I). The gabbroic contribution locally reaches almost 100% of the rock. In this case, its detrital origin, instead of larger metagabbro slices, can be safely confirmed only in this section, where disrupted fragments of igneous pyroxene and plagioclase, now replaced by lawsonite aggregates, are associated with minor Ca-carbonate and organic matter, indicating a sedimentary mixing. The Bisinchi metaconglomerate sliver is nowadays covered by thick vegetation, and a detailed characterization was not possible during our survey. Similar metaconglomerate lenses are found in the blueschist units of the Western Alps (e.g. Rocher Blanc breccias, Caby et al., 1971).

Continental basement slivers consisting of ortho- and paragneiss are locally found atop of the mafic/ultramafic ophiolitic basement (Fig. 3B, D), and are interpreted as continental extensional allochthons (Meresse et al., 2012; Vitale Brovarone et al., 2011b and references therein). In the studied area, one slice of continental basement rocks occurs in the proximity of the Campitello village, and also comprises a Triassic dolomitic cover (Fig. 2A; Rossi et al., 2002). As noticed for the continent-derived conglomeratic lenses, continental basement slivers intercalated within the Schistes Lustrés of the BSZ are systematically found in the lower part of the unit, close to the contact with the EZ.

3.2. Eclogite zone (EZ)

The EZ mostly consists of dominant metaophiolites including serpentinites, metabasalts and metagabbros, together with continental-basement and metasedimentary rocks, including metacherts, marbles and calcschists. The EZ in the study area represents the northern and more intensely deformed prolongation of the San Petrone units. The tectonostratigraphy of this unit is extremely variable, and more details can be found in Vitale Brovarone et al. (2011b). Serpentinites are variably deformed and locally preserve primary peridotite textures. Ophicarbonates do not occur in the study area, but are found southward in the same tectonometamorphic unit. Metagabbros are rare and occur as relatively small bodies within or capping serpentinites.

Fig. 3. Ophiolitic metabreccias and blocks of the BSZ. A) Panoramic view of the Bigorno pass area. Note the occurrence of ophicarbonate capping the ultramafic basement, indicating the preservation of an oceanic detachment surface. B) Ophiolitic metabreccia at the Bigorno pass. As for most metabreccias in the BSZ, this layer mostly consists of gabbroic or microgabbroic clasts (C) and minor ophicarbonate clasts (B). D) Chlorite–ankerite-rich horizon within metapelites of the BSZ (Morosaglia). E) Basaltic metabreccia within metapelite. F) Detail of a large metagabbro boulder included in metapelites. Note the occurrence of a basaltic dyke (upper part of the photo) crosscutting the gabbro.



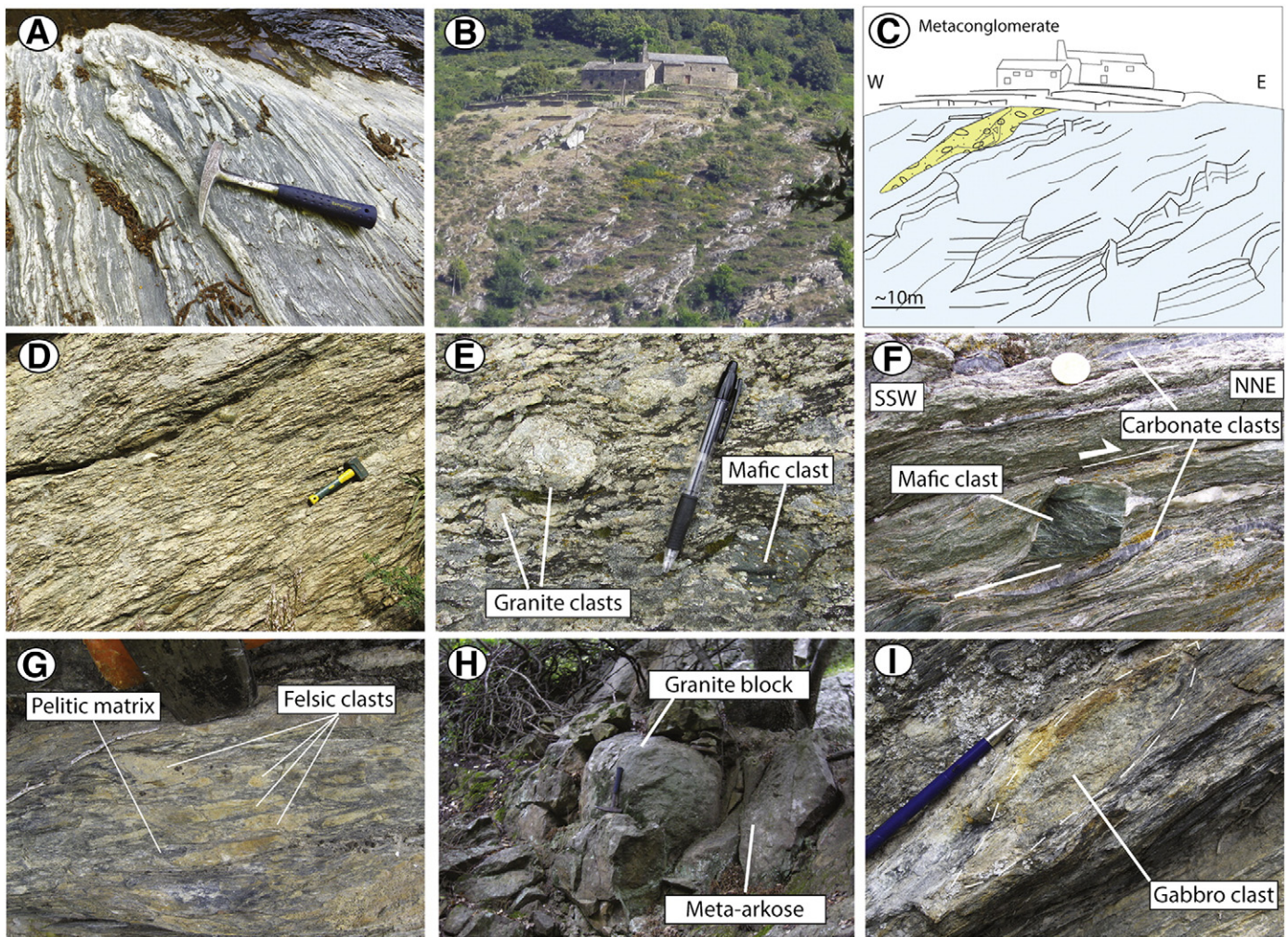


Fig. 4. Metasedimentary cover rocks of BSZ. A) Typical outcrop of metapelite in the BSZ. B, C) Panoramic view (B) and line drawing (C) of the Santa Reparata metaconglomerate (Morosaglia, Fig. 2B). D, E, F) Santa Reparata metaconglomerate. Note the abundance of acidic clasts (E) and the local occurrence of mafic (E, F) and carbonate clasts (F) in the arkosic matrix. In F, note the top-to-the-NNE sense of shear defined by the mafic clast. G, H, I) Castello di Rostino metaconglomerate. In G, acidic clasts embedded in metapelitic matrix. In H, metric granitic boulder included in arkosic matrix. In I, gabbroic clast in the metaconglomerate.

Metabasalts form a thick and rather continuous body that frequently preserves pillow and pillow breccia textures. This body, which crops out in the eastern part of the unit, runs all along Alpine Corsica and form the so-called Mandriale unit (Lahondère et al., 1999). Primary textures are preserved down to the microscale, with aphyric, vitrophyric and porphyritic textures replaced by HP minerals such as glaucophane, omphacite, lawsonite and garnet (cf. also Vitale Brovarone et al., 2011a). Almost undeformed pillow metabasalts are observed in large loose boulders occurring in the area of Castello di Rostino (Fig. 5A). In the same area, intensely deformed and boudinaged metabasalts are found as rounded boudins within metasedimentary rocks (see Discussion). A large part of the metabasaltic rocks represent former volcano-sedimentary deposits comprising isolated pillows and pillow fragments (Fig. 5B). Based on their stratigraphic position, at the base of the metasedimentary pile, these detritic rocks represent the early sediments capping the mafic-ultramafic basement.

Continent-derived material, including both slivers of basement rocks and acidic metaconglomerates (e.g. Accendi Pipa slices, Lahondère, 1996), is locally found in contact with serpentinites, and is interpreted as a primary lithological association of a Mesozoic OCT zone (Vitale Brovarone et al., 2011b). A new slice of continental basement rocks was discovered during our survey in the area of Bocca di Bruno (Fig. 2).

This composite basement is capped by a metasedimentary cover with stratigraphic lateral variations. Metachert is found as the lowest

stratigraphic lithology overlying metabasalts or serpentinites, but is discontinuous. Unlike most metachert of the BSZ, in the EZ it contains small, Mn-rich garnet, as observed in HP radiolarian metacherts from the cover of the Pelvas d'Abries gabbros in the Western Alps (Ballèvre and Lagabrielle, 1994). Impure marbles follow metachert upward, but are only locally observed. Calcschists represent the dominant metasedimentary rock (Fig. 5C). As a whole, the EZ metasedimentary sequence is richer in carbonate-rich metasedimentary rocks (i.e. calcschists) compared to the metapelite-rich BSZ.

4. Alpine deformation

A detailed characterization of the deformation patterns of the Nappes Supérieures units in the studied area is beyond the aim of this paper, and only some general aspects of its contact with the BSZ are herein highlighted. The internal structure of the Nappes Supérieures and its juxtaposition with the HP units of the Schistes Lustrés (BSZ-EZ) is characterized by a top-to-the-west extensional deformation defined by high-angle shear bands. The contact separating the Caporalino-Pedani unit from the underlying ophiolites is defined by highly sheared serpentinites. This contact is best exposed at the Bocca a Serna pass (Fig. 2B). The contact that separates the weakly metamorphosed ophiolites of the Nappes Supérieures from the HP Schistes Lustrés is exposed along the D71 road (Fig. 2B). It separates

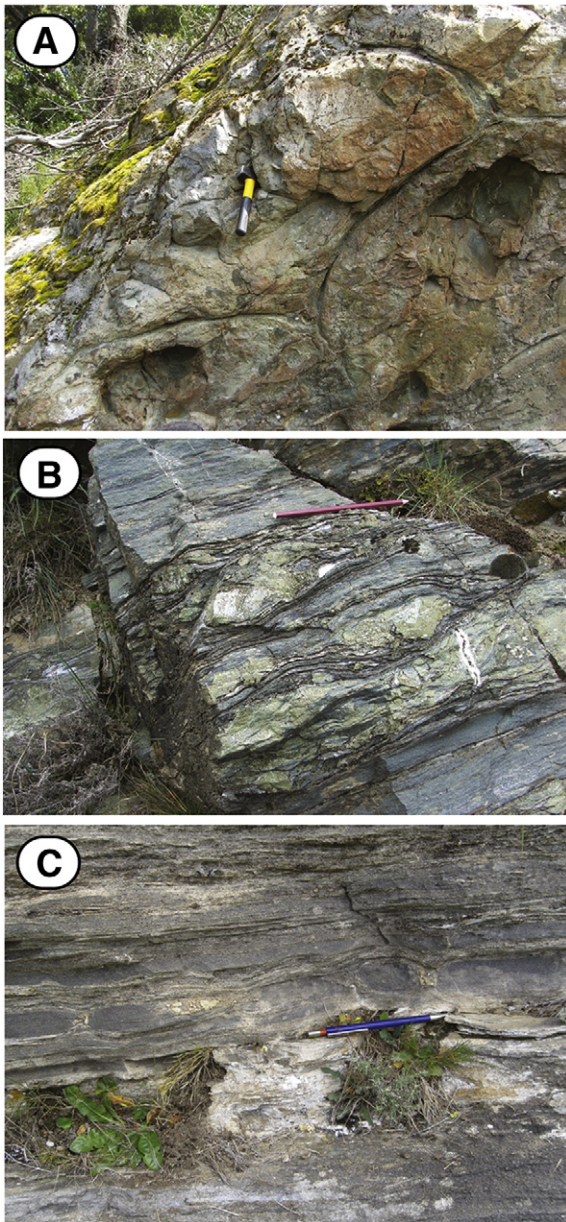


Fig. 5. Metabasalts and cover rocks of the EZ. A) Well-preserved pillow basalt (Castello di Rostino ridge). Note that this metabasalt is fully recrystallized at lawsonite–eclogite-facies conditions. From [Vitale Brovarone et al. \(2011a\)](#). B) Typical facies of EZ volcano-sedimentary metabasites (Monte Compoli). Variably dismembered pillow basalts are embedded in a tuffitic matrix. These rocks form a thick body extending N–S all along alpine Corsica, the so-called Mandriale unit ([Lahondère et al., 1999](#)). C) Typical outcrop of the EZ Calcschists. Note the abundance of carbonate layers.

subgreenschist-facies metabasalts of the Nappes Supérieures from blueschist-facies metasedimentary rocks of the BSZ, and shows brittle–ductile deformation in basalts of the former and ductile deformation in metasedimentary rocks of the latter, with a top-to-west kinematics likely associated with extensional deformation along the western flank of the Schistes Lustrés antiform.

Structures of the BSZ and EZ result from a polyphasic evolution characterized by non-coaxial deformation and leading to the formation of a general west-dipping composite fabric in the studied area, i.e. the western flank of the Schistes Lustrés antiformal stack (Figs. 6, 7 and 8). This composite fabric can be subdivided into three main tectonometamorphic events representative of prograde/peak and retrograde HP conditions (HPp and HPr, respectively) and late low-P conditions (LP) (see next sections for metamorphic details; Fig. 6). Structures associated with the

two HP condition events are parallelized and almost undistinguishable in the field (Fig. 7).

In the BSZ, the occurrence of a progressive eastward metamorphic gradient (cf. next section) is accompanied by the progressive development and distribution of HPp structures, and a general eastward strain gradient (Fig. 8). The primary compositional layering alternating metapelites with marbles is progressively transposed by a west-dipping crenulation cleavage, whose spacing progressively decreases toward the east. In the eastern part of the BSZ, the primary lithological layering is intensely transposed by tight isoclinal folding. The geometrically oldest structures associated with this transposition define non-cylindrical, intrafolial isoclinal folds alternating lepidoblastic layers and granoblastic layers, or, at a larger-scale, is characterized by the local preservation of tight marble fold hinges (Fig. 6B). In more intensely deformed samples, relicts of this phase are limited to intrafolial microlithons observed in thin section (see Section 5.3). Stretching lineations associated with HP mineral phases (e.g. blue amphibole, see next section) are oriented NNE–SSW, and parallel to the measured fold axes (Fig. 7). Axial planes are parallelized to the main regional fabric.

The HPp fabrics are transposed by and progressively rotated into parallelism with the HPr deformation, which is characterized by a second generation of non-cylindrical isoclinal folds/fabrics showing orientations as phase HPp (Fig. 7). Metachert best preserves primary intersections between the two fabrics (Fig. 6C). Event HPr is responsible for a penetrative axial-plane foliation.

The study of deformation in metaophiolites of the BSZ, which mostly occur as block in a metasedimentary matrix, is more complex and affected by progressive rotation. Fabrics associated with HPp mineral assemblages, such as Na-amphibole and lawsonite, are generally parallel to their equivalent in the enclosing metasedimentary matrix, and suggest a common evolution. Fold orientation within metaophiolite block is more scattered, and probably results from rotation during deformation. Shear sense is best defined in the Morosaglia metaconglomerate, where acidic and mafic clasts clearly indicate a top-to-NE kinematics (Fig. 4F).

In the EZ, HPp deformation and assemblages are best preserved in metabasites, and locally form a penetrative fabric associated with lawsonite-facies assemblages (see next section). Stretching lineations are oriented NNE–SSW, and concordant with those of the BSZ (Fig. 7). Fold axes show similar orientations but are more scattered, testifying for non-cylindrical deformation (Fig. 7). Axial planes dip to the west with a slightly lower angle compared to the BSZ, and reflect a position closer to the hinge of the large antiformal stack. The rotation of pillow clasts in volcano-sedimentary rocks, mostly suggests a top-to-NE sense of shear. Calcschists are characterized by the same progressive deformation from HPp to HPr observed in the BSZ. The progressive transition from HPp to HPr is responsible for the large-scale geometries defined by the lithological boundary separating the main metaophiolite sheet and the overlying metasedimentary cover. These structures form large, east-oriented isoclinal folds, cored by serpentinites or metabasalts (Fig. 8), and characterized by NNE–SSW axes and N-oriented stretching lineations, together with a penetrative west-dipping schistosity (Fig. 8).

The contact zone between the BSZ and EZ is characterized by intense shear. Rocks of the BSZ show a progressive strain gradient toward the contact. More distinct deformation patterns characterize the EZ along this contact, and affect both calcschists and metaophiolites. HPr isoclinal fold hinges in metaophiolite sheet are intensely boudinaged and result in a tectonic block-in-matrix structure that was not observed far away from the contact zone (Fig. 8A; see also Discussion). This shear zone is associated with rather gentle NNE–SSW oriented stretching lineations, but a sound kinematic characterization was not clearly established during our survey.

LP deformation shows common features in both the BSZ and EZ, and comprises structures characterized by the development of open folds associated with a non-penetrative schistosity mainly associated with high-angle shear bands. This deformation is locally penetrative and slightly discordant with the main HP fabrics, especially in the EZ,

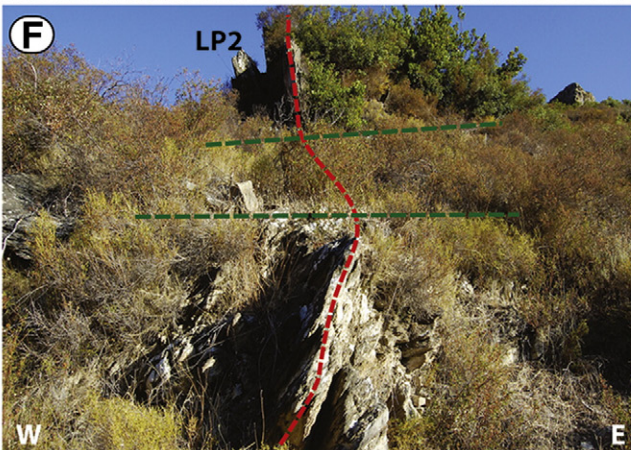
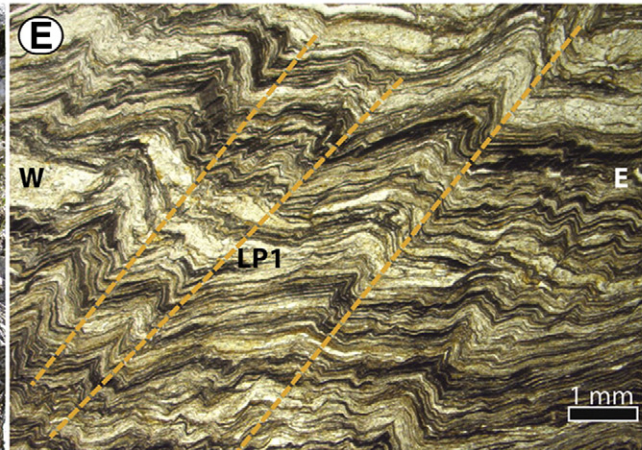
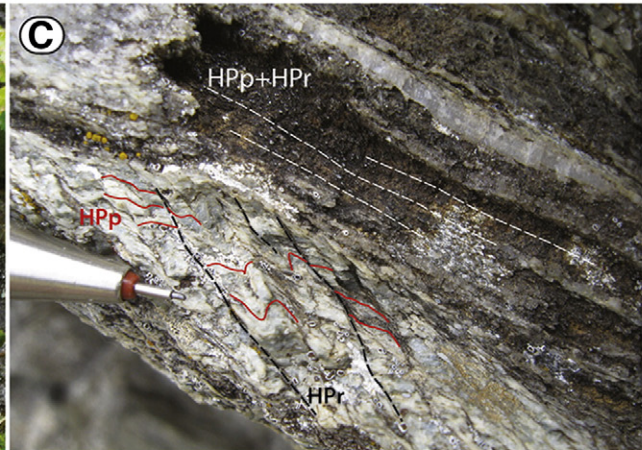
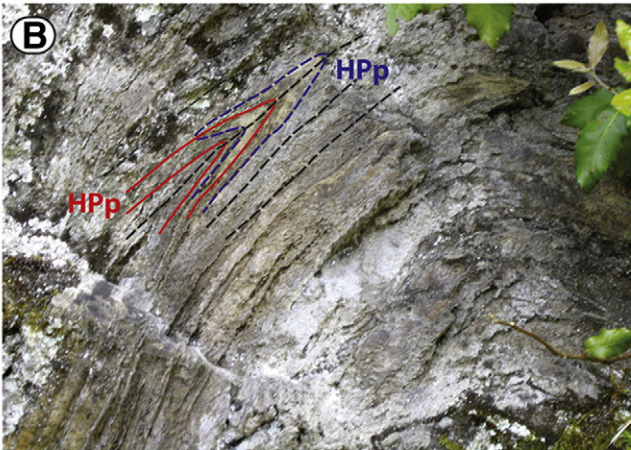
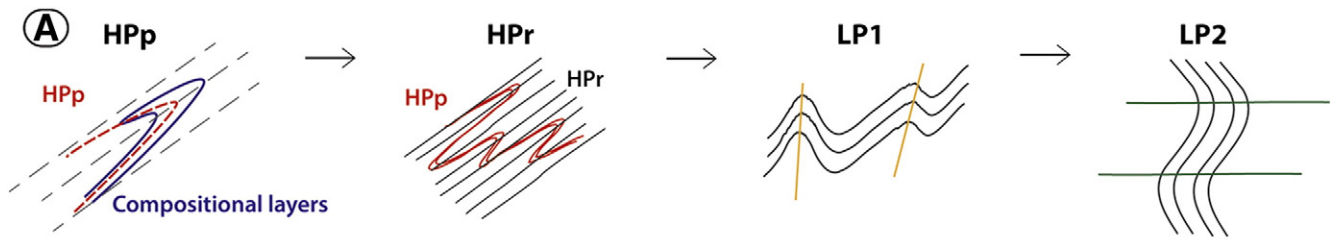


Fig. 6. A) Schematic cartoon showing the most characteristic meso-structures and deformation styles of HP and LP tectonometamorphic stages in Alpine Corsica. B) Example of relicts of HPp structures. In this case, a HPp isoclinal fold defined by primary compositional layers is successively refolded during the HPr stage. C) Example of geometrical relationships between HPp and HPr fabrics. Note the distinct discordance of HPp and HPr fabrics in the more competent metacherts (lower part), and the complete transposition and parallelization of the two fabrics in the less competent terrigenous metasedimentary rocks. D, E) Example of LP open folds associated with a poorly penetrative, high-angle schistosity. In (E) (thin section, plane-polarized light – PPL), note the absence of a well-developed schistosity in these structures. F, G) Examples of LP open folds characterized by flat axial planes and the absence of axial plane schistosity.

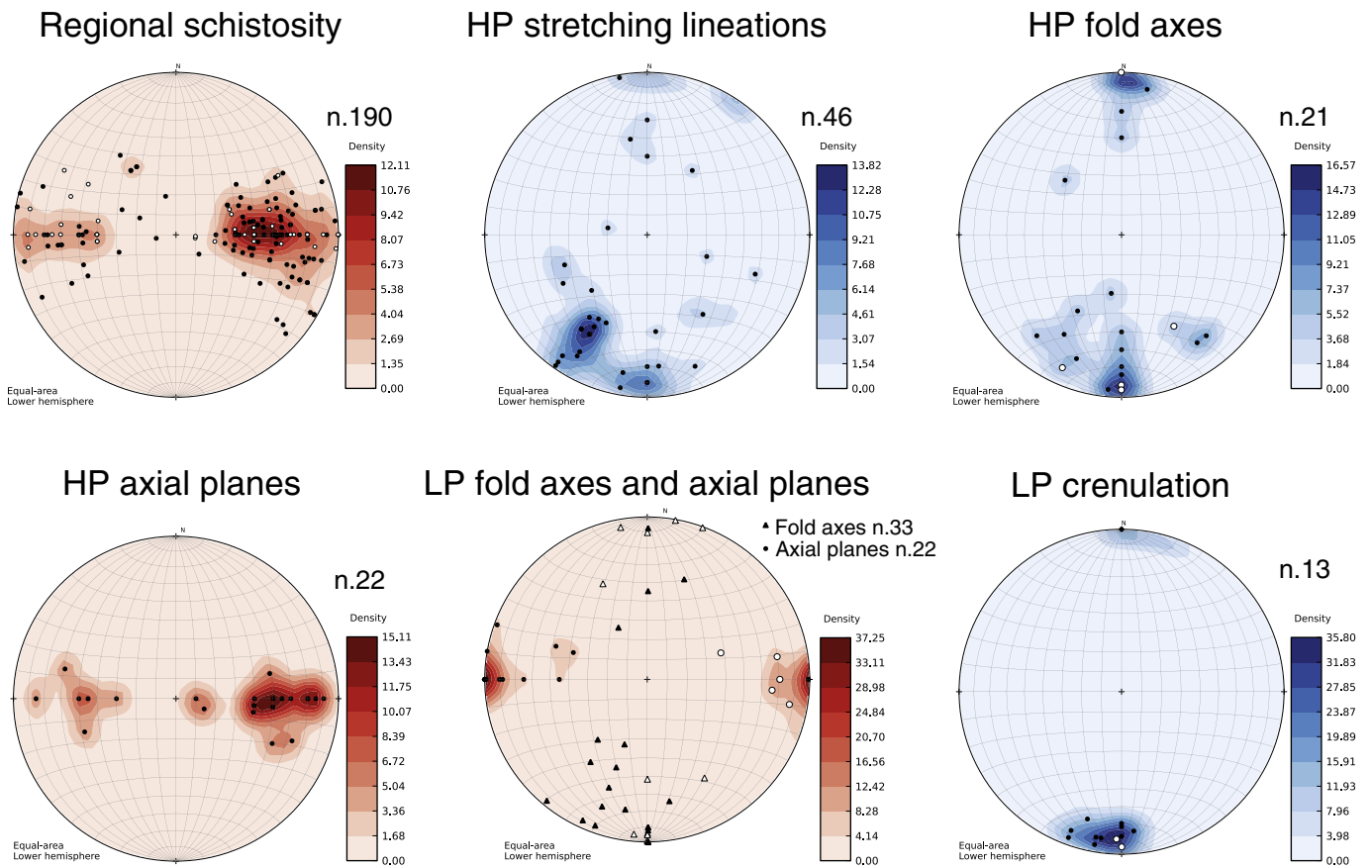


Fig. 7. Lower hemisphere Schmidt projection plots of structural elements in the studied area. High-pressure prograde (HPp) and retrograde (HPr) data are concordant and plotted together. Black and white symbols refer to BSZ and EZ structural data, respectively.

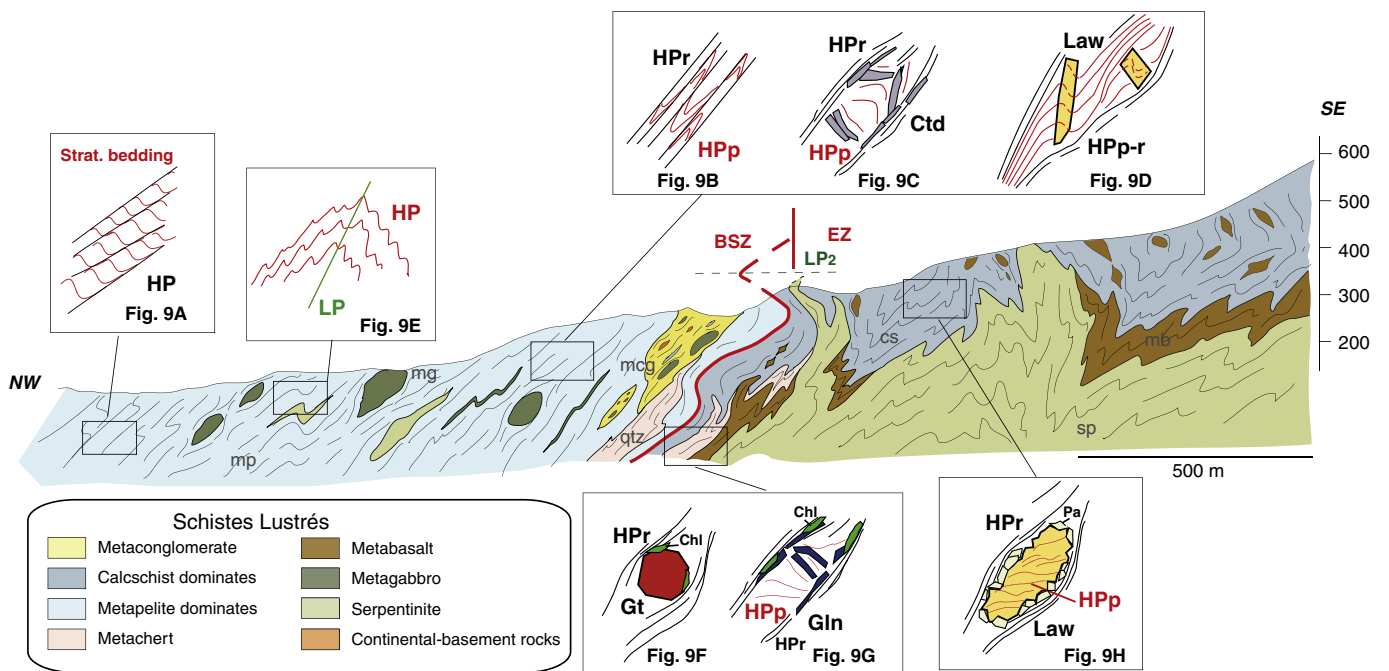


Fig. 8. Interpretative geological cross-section across the BSZ and EZ zones (see Fig. 2B for location). The most representative microstructural relationships of the HP phases are schematically drawn (see Fig. 9 for details and microphotographs).

where HP fabrics are less steep due to their occurrence in the hinge of the Schistes Lustrés antiform. Two generations of late folding are characterized by vertical and horizontal axial planes, respectively (Figs. 6, 7). The first generation is often associated with a poorly penetrative crenulation cleavage, and shows ~NS fold axes (Figs. 6D, E, 7). It may represent a local expression of the main Schistes Lustrés antiformal structure. The second generation forms large recumbent folds responsible for the local, westward rotation of the regional schistosity and associated east-dipping foliation (Figs. 6E, F, 7). This latter folding also affects the contact separating the BSZ and EZ (Fig. 8A).

Late, high-angle normal faults were locally found, especially in the contact zones between the Nappes Supérieures and the BSZ and along the BSZ–EZ boundary (Fig. 2B).

5. Petrography and mineral chemistry

5.1. Analytical parameters for mineral chemistry

Representative analyses of the studied minerals are reported in Table 2. The mineral analyses were performed using a Cameca SX-Five and a Cameca SX-100 electron microprobes (Camparis, Univ. Paris 6). Classical analytical conditions were adopted for spot analyses [15 kV, 10 nA, wavelength-dispersive spectroscopy (WDS) mode], using Fe₂O₃ (Fe), MnTiO₃ (Mn, Ti), diopside (Mg, Si), CaF₂ (F), orthoclase (Al, K), anorthite (Ca) and albite (Na) as standards. Quantifications were derived from the automated Cameca ZAF quantification procedure.

5.2. Patterns of metamorphism in the study area

The very low-grade, subgreenschist-facies metamorphic patterns of the Nappes Supérieures zone are beyond the scope of this paper, and only a few thermometric estimates are included in this study (Figs. 10 and 11).

The BSZ is characterized by a gradual eastward increase of metamorphism that, in metasedimentary rocks, corresponds to a progressive increase of the grain-size of lepidoblastic layers, together with the increase of the Si_{a,p,f,u} content in phengite and the appearance of successive mineral isograds (see also representative mineral assemblages in Table 1). Carpholite was found in the western and lower-grade part of

the BSZ (village of Ponte Novo). Further to the east, chloritoid appears as small crystals in metapelites and defines a north–south-oriented isograd (Fig. 10). Retrogression is scarce and generally static in metabasites and metasedimentary rocks and attested by large albite porphyroblasts, chlorite on former Na-amphibole and pseudomorphic epidote/paragonite aggregates on lawsonite.

Lawsonite in metabasites is common all over the BSZ and EZ, and thus does not represent a diagnostic mineral. Na-amphibole is common in metabasites, and varies in composition eastward from Mg-riebeckite to glaucophane and based on the selected lithology (Fe³⁺-rich-poor). Omphacite veins are commonly found in metagabbro bodies in the eastern part of the BSZ, and point to P conditions above the albite = jadeite + quartz reaction (Vitale Brovarone, 2013). In metasedimentary rocks, the appearance of lawsonite is in most cases due to HP metamorphic processes (Vitale Brovarone et al., 2014), and defines a regional north–south-oriented contour (Fig. 10).

The BSZ–EZ boundary corresponds to the appearance of garnet in both metachert and metabasites. Importantly, garnet was not observed in any rock type of the BSZ. Omphacite, lawsonite and glaucophane also characterize metabasites of the EZ, and testify for lawsonite–eclogite-facies conditions (Table 1). Epidote in metabasites occurs both in retrograde assemblages and, together with lawsonite, in the peak-metamorphism parageneses in intensely deformed volcano-sedimentary, Fe³⁺-rich layers (pistacite-rich). Calc schists of the EZ are poorly diagnostic, and only locally retain relicts of lawsonite, Na-amphibole and more rarely, chloritoid, together with high-Si content in phengite (~3.5–3.6 a.p.f.u., Table 2). In some samples, fully retrogressed lawsonite is recognized by preserved CM trails in lozenge-shaped paragonite aggregates.

5.3. Microstructural relationships

In this section we focus on the microstructural evolution of metasedimentary rocks of the Blueschist and Eclogite zones. Metabasites were not considered because in the BSZ they mainly occur as blocks within a metasedimentary matrix and may have experienced rotation during deformation, which makes correlations with the regional structural data in the host metasedimentary rocks difficult to be established.

Table 1 Representative mineral assemblages in metasediments and metabasites of the BSZ and EZ during HPP, HPr and LP conditions. ± indicates phases that may be present depending on the selected sample. Note that the assemblages for each stage refer to the average metasedimentary or metabasic suites, and may not occur all in the same sample. Ferric epidote may occur in lawsonite bearing metabasites, and does not imply lawsonite breakdown. Si content in phengite (a.p.f.u.) is also reported for the different stages, while measured. Lawsonite in the BSZ appears at T > 360 °.

	BSZ (western zone, 350–400 °C)			BSZ (eastern zone, 400–470 °C)			EZ		
	HPP	HPr	LP	HPP	HPr	LP	HPP	HPr	LP
<i>Metasediments</i>									
Quartz	-----	-----	-----	-----	-----	-----	-----	-----	-----
Phengite			3.1–3.2	3.4–3.5	3.3–3.4	3.1–3.2	3.5–3.6	3.4–3.5	3.1–3.2
Ca-carbonate	±	±	±	±	±	±	±	±	±
Carpholite	-----								
Chloritoid				X _{Mg} 0.7–0.11	?			?	
Chlorite	-----	-----	-----		-----	-----		-----	-----
Lawsonite	>360 °C	-----	?	-----	-----	?	-----	-----	-----
Garnet									
Blue amphibole				-----	?		-----	?	
<i>Metabasites</i>									
Quartz	±	±	±	±	±	±	±	±	±
Phengite	±	±	±	±	±	±	3.5–3.6	3.4–3.5	
Ca-carbonate							±	±	±
Omphacite				-----			-----	?	
Lawsonite	-----	---		-----	---		-----	?	
Garnet									
Epidote	Fe ³⁺	Fe ³⁺	-----	Fe ³⁺	Fe ³⁺	-----	Fe ³⁺	-----	-----
Chlorite	±	-----	-----	±	-----	-----	±	-----	-----
Blue amphibole	-----	-----	-----	-----	-----	-----	-----	-----	-----
Green amphibole	-----	-----	-----	-----	-----	-----	±	±	-----

Table 2

Representative analyses of chloritoid, phengite, amphibole and garnet of selected samples for PT estimates. Phengite analyses refer to HPP assemblages.

	Chloritoid	Chloritoid	Chloritoid	Chloritoid	Chloritoid	Chloritoid	Chloritoid	Chloritoid		Phengite	Phengite	Phengite	Phengite	Phengite	Phengite	Phengite	Phengite
	OF3745	OF3745	OF3745	OF3778	OF3778	OF3778	OF3778	OF3778		OF3778	OF3778	OF3745	OF3745	OF3698	OF3698	OF3781	OF3781
SiO ₂	23.2	24.1	23.7	24.07	24.04	24.06	24.03	24.12	SiO ₂	50.87	51.95	52.03	51.73	52.15	51.37	50.35	50.34
TiO ₂	0.0	0.1	0.0	0.04	0.00	0.03	0.04	0.00	TiO ₂	0.05	0.10	0.11	0.09	0.12	0.04	0.14	0.16
Al ₂ O ₃	39.8	39.7	40.2	41.14	40.50	40.34	40.81	40.77	Al ₂ O ₃	27.45	28.88	26.94	26.71	26.61	26.26	29.10	29.49
FeO	25.2	25.0	26.0	25.94	25.69	25.86	25.14	25.89	FeO	2.93	3.15	3.93	3.80	3.89	3.64	3.85	3.84
MnO	0.7	0.9	0.9	0.83	0.76	0.75	0.79	0.82	MnO	0.02	0.03	0.04	0.02	0.02	0.04	0.01	0.02
MgO	1.4	1.5	1.3	1.08	1.16	1.09	1.11	1.01	MgO	2.95	2.87	2.91	2.98	2.97	3.05	2.22	2.12
CaO	0.0	0.0	0.0	0.00	0.03	0.02	0.02	0.03	CaO	0.01	0.04	0.04	0.02	0.01	0.00	0.04	0.06
Na ₂ O	0.0	0.0	0.0	0.00	0.01	0.03	0.03	0.04	Na ₂ O	0.32	0.17	0.18	0.27	0.21	0.16	0.28	0.33
K ₂ O	0.0	0.0	0.0	0.03	0.01	0.03	0.02	0.00	K ₂ O	10.03	8.72	10.00	9.87	9.91	10.18	9.83	9.92
Total	90.5	91.3	92.2	93.13	92.20	92.23	91.99	92.67	Total	94.64	95.91	96.19	95.50	95.89	94.74	95.82	96.29
Si	2.0	2.0	2.0	1.99	2.01	2.01	2.01	2.01	Si	3.41	3.41	3.45	3.45	3.46	3.46	3.35	3.33
Ti	0.0	0.0	0.0	0.00	0.00	0.00	0.00	0.00	Ti	0.00	0.00	0.01	0.00	0.01	0.00	0.01	0.01
Al	4.0	3.9	4.0	4.01	3.99	3.98	4.02	4.00	Al	2.17	2.23	2.10	2.10	2.08	2.08	2.28	2.30
Fe ⁺³	0.0	0.0	0.0	0.00	0.00	0.00	0.00	0.00	Fe ⁺³	0.00	0.00	0.00	0.00	0.00	0.00	0.00	0.00
Fe ⁺²	1.8	1.8	1.8	1.80	1.80	1.81	1.76	1.80	Fe ⁺²	0.16	0.17	0.22	0.21	0.22	0.20	0.21	0.21
Mn	0.1	0.1	0.1	0.06	0.05	0.05	0.06	0.06	Mn	0.00	0.00	0.00	0.00	0.00	0.00	0.00	0.00
Mg	0.2	0.2	0.2	0.13	0.14	0.14	0.14	0.13	Mg	0.29	0.28	0.29	0.30	0.29	0.31	0.22	0.21
Ca	0.0	0.0	0.0	0.00	0.00	0.00	0.00	0.00	Ca	0.00	0.00	0.00	0.00	0.00	0.00	0.00	0.00
Na	0.0	0.0	0.0	0.00	0.00	0.01	0.00	0.01	Na	0.04	0.02	0.02	0.03	0.03	0.02	0.04	0.04
K	0.0	0.0	0.0	0.00	0.00	0.00	0.00	0.00	K	0.86	0.73	0.85	0.84	0.84	0.87	0.83	0.84
OH	4.0	4.0	4.0	4.00	4.00	4.00	4.00	4.00	OH	2.00	2.00	2.00	2.00	2.00	2.00	2.00	2.00
XMg	0.1	0.1	0.1	0.07	0.07	0.07	0.07	0.07									
XFe	0.9	0.9	0.9	0.93	0.93	0.93	0.93	0.93									

OF3704																	
	Actinolite	Actinolite	Actinolite	Glauco-phane	Glauco-phane	Glauco-phane	Na-Ca glauc.	Na-Ca glauc.	Phengite	Phengite		Garnet rim	Garnet rim	Garnet rim	Garnet core	Garnet core	Garnet core
SiO ₂	57.18	55.13	55.67	59.21	59.22	58.84	57.68	57.54	52.73	53.50	SiO ₂	37.06	37.3	37.11	37.27	37.26	36.97
Al ₂ O ₃	0.65	1.92	1.02	9.94	9.62	9.38	6.26	6.40	22.87	17.14	Al ₂ O ₃	19.56	19.21	19.43	19.33	19.44	19.45
FeO	14.20	14.89	14.06	13.73	13.93	14.15	18.94	17.60	5.26	7.37	Fe ₂ O ₃	2.75	2.65	2.77	2.32	2.11	2.88
MgO	15.10	13.96	14.76	8.97	9.31	9.03	8.50	9.15	3.70	6.48	FeO	25.3	25.31	25.68	23.49	23.83	23.45
CaO	12.09	9.93	11.47	0.31	0.32	0.62	1.46	1.48	0.00	3.26	MnO	5.5	5.35	5.46	8.08	8.18	8.2
Na ₂ O	0.68	1.72	0.95	6.68	6.60	6.49	6.00	5.93	0.00	0.35	MgO	1.01	0.97	1.12	0.83	0.8	0.95
K ₂ O	0.01	0.01	0.01	0.01	0.01	0.01	0.01	0.01	11.02	7.49	CaO	9.09	9.48	8.72	8.91	8.6	8.4
Total	98.79	97.58	98.31	98.87	99.03	98.54	98.87	98.13	95.57	95.59	Total	100.27	100.27	100.29	100.23	100.21	100.3
Si	7.99	7.92	7.97	8.06	8.05	8.06	8.07	8.06	3.56	3.64	Si	2.99	3.01	2.99	3.01	3.01	2.99
Al	0.11	0.32	0.17	1.60	1.54	1.51	1.03	1.06	1.82	1.37	Al	1.86	1.83	1.85	1.84	1.85	1.85
Fe3	0.03	0.28	0.11	0.42	0.53	0.44	0.77	0.77	0.00	0.00	Fe ³⁺	0.17	0.16	0.17	0.14	0.13	0.18
Fe2	1.66	1.47	1.56	1.10	1.00	1.13	1.36	1.20	0.30	0.42	Fe ²⁺	1.71	1.71	1.73	1.59	1.61	1.58
Mg	3.21	2.99	3.15	1.82	1.89	1.85	1.77	1.91	0.37	0.66	Mn	0.38	0.37	0.37	0.55	0.56	0.56
Ca	1.85	1.53	1.76	0.04	0.05	0.09	0.22	0.22	0.00	0.24	Mg	0.12	0.12	0.13	0.10	0.10	0.11
Na	0.19	0.48	0.26	1.76	1.74	1.73	1.63	1.61	0.00	0.05	Ca	0.79	0.82	0.75	0.77	0.74	0.73
K	0.00	0.00	0.00	0.00	0.00	0.00	0.00	0.00	0.95	0.65	X _{Ca}	0.25	0.26	0.24	0.24	0.24	0.23
OH	2.00	2.00	2.00	2.00	2.00	2.00	2.00	2.00	2.00	2.00	X _{Fe}	0.59	0.59	0.60	0.55	0.55	0.56
											X _{Mg}	0.04	0.04	0.04	0.03	0.03	0.04
											X _{Mn}	0.12	0.12	0.12	0.18	0.18	0.18

5.3.1. Blueschist zone

Metapelites were selected for microstructural analysis in thin section because they provide the best constraints between deformation and diagnostic mineral assemblages (e.g. phengite, carpholite, chloritoid, Table 1). The studied metapelite samples (OF3781, OF3778, OF3745, OF3698) display a composite foliation resulting from the superposition of HP(p, r) and LP fabrics. In the lower-grade part of the BSZ, a distinct Alpine fabric results from the folding and transposition of thin compositional layers, probably representing the primary stratigraphic bedding (Fig. 9A). Carpholite-bearing veins cut across this fabric but are also deformed within it, possibly indicating a transitional stage between HPP and HPr conditions.

In the eastern and higher-grade zone of the BSZ, rocks show much complex polyphased microstructural features. The dominant foliations result from the intense transposition of HP fabrics, relicts of which are preserved in stretched isoclinal folds hinges (Fig. 9B) and in microlithons. The latest HP deformation (HPr) consists of a penetrative axial plane foliation that can be only locally distinguished from the older intensely transposed ones (HPP). The distinction between HPP and HPr fabrics often proves difficult, especially in the western and lower-grade part of the unit. Relicts of the highest-grade HPP metamorphic conditions (highest substituted phengite, chloritoid) are mostly concentrated in microlithons whose minerals are oriented not only at high angle to the main foliation, but they also occur parallel to it (e.g. samples OF3778 and OF3745, Fig. 9C). In the case of phengite, the main schistosity comprises both highly substituted and weakly substituted compositions, indicating a polyphased evolution at different P–T conditions. Single phengite crystals within the main schistosity exhibit scattered compositional patterns without diagnostic zoning, e.g. highly substituted (Si a.p.f.u.) cores and weakly substituted rims. However, due to the clear preponderance of highly substituted (i.e. higher P–T) in older microstructural sites (e.g. microlithons, fold hinges), we assume that the highly substituted phengite domains in the main fabric represent relicts of HPP conditions. Lawsonite is syn-kinematic with respect to the HPP schistosity, and successively rotated during the HPr and LP events (Fig. 9D). Fresh lawsonite was also found in metapelites very close to the contact with the EZ. Low pressure deformation commonly occurs as open folds and shear bands leading to a weak and poorly penetrative fabric (Fig. 9E).

5.3.2. Eclogite zone

Metasedimentary rocks of the EZ show not only similar patterns relative to the BSZ, such as the occurrence of superimposed HP and LP fabrics, but also some relevant contrasts. The peak HP mineralogy, i.e. high Si phengite, garnet, glaucophane, lawsonite (Table 1), is preserved in microlithons and intensively transposed fabrics (Fig. 9F, G). Relicts of the highest substituted phengites (3.5–3.6 a.p.f.u.), i.e. highest HPP conditions, are best preserved in microlithons wrapped around by HPr/LP fabrics characterized by lower P phengites (Si = 3.4–3.2 a.p.f.u.). Blue amphibole, glaucophane in most cases, and garnet are partially replaced by chlorite during the HPr and LP stages, either dynamically or statically. The main difference between the two zones, apart from the occurrence of higher-grade minerals such as garnet, is the more distinct destabilization of lawsonite during the development of the HPr schistosity (Fig. 9H). Lawsonite in some cases preserves traces of the earlier HPP fabrics defined by inclusions of carbonaceous material and rutile (Fig. 9H).

6. Constraining metamorphic conditions

6.1. Raman spectroscopy of carbonaceous material (RSCM)

RSCM thermometry provides maximum temperature estimates (T_{\max}) for carbonaceous-rich samples, based on the irreversible transformation of organic matter during metamorphism (Beysac et al., 2002; Lahfid et al., 2010). Raman spectra were obtained using a Renishaw InVIA Reflex microspectrometer (IMPMC Paris). We used a 514 nm Laser Physics argon laser in circular polarization. The laser was focused on the sample by a DMLM Leica microscope with a 100× objective (NA = 0.85), and the laser power at the sample surface was set around 1 mW. The Rayleigh diffusion was eliminated by edge filters, and to achieve nearly confocal configuration the entrance slit was closed down to 15 μm. The signal was finally dispersed using a 1800 gr/mm grating and analyzed by a Peltier cooled RENCAM CCD detector. Before each session, the spectrometer was calibrated with a silicon standard. Because Raman spectroscopy of CM can be affected by several analytical mismatches, we closely followed the analytical and fitting procedures described by Beysac et al. (2002, 2003). Measurements were done on polished thin sections cut perpendicularly to the main fabrics and CM was systematically analyzed below a transparent adjacent mineral, generally quartz. 10–20 spectra were recorded for each sample in the extended scanning mode (1000–2000 cm^{-1}) with acquisition times from 30 to 60 s. Spectra were then processed using the software Peakfit (following Beysac et al., 2002). Based on the obtained spectra, T from samples characterized by lower-T metamorphism (i.e. $\sim 200 < T < 350$ °C) were estimated using the correlation proposed by Lahfid et al. (2010). At higher-T (i.e. $\sim 350 < T < 650$ °C) T was calculated using the calibration of Beysac et al. (2002), with a calibration-attached accuracy of ± 50 °C due to uncertainties on petrologic data used for the calibration. Relative uncertainties on T are, however, much smaller, around 10–15 °C (Beysac et al., 2004).

6.2. Pseudosections

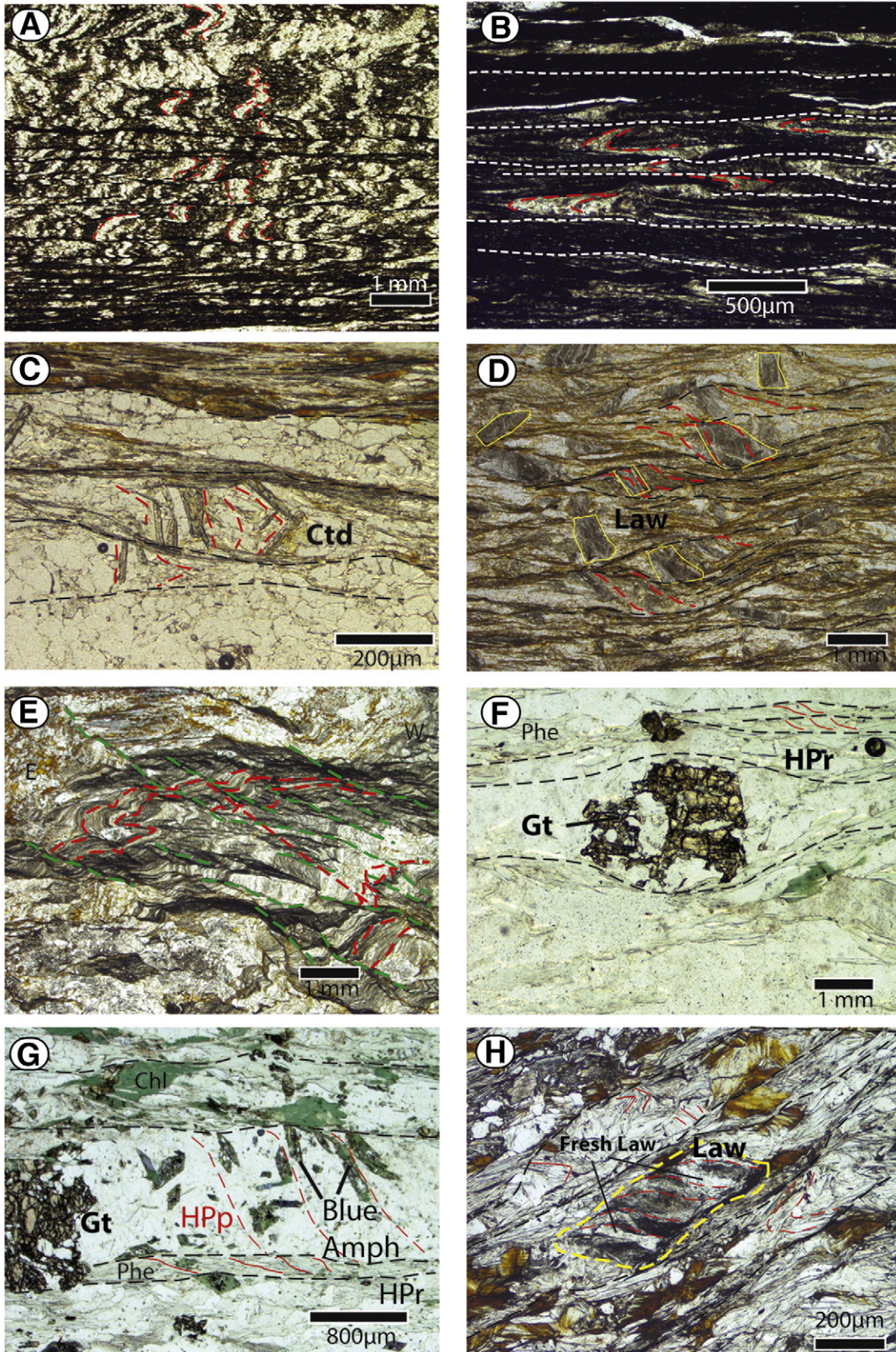
Pseudosections were calculated using Perple_X (07 version, Connolly, 2009). Metasedimentary samples were modeled in the system K_2O – FeO – MgO – Al_2O_3 – SiO_2 – H_2O (KFMASH) system. Bulk compositions were obtained using a Zeiss ULTRA scanning electron microscopy (SEM) coupled with field emission gun (FEG) at IMPMC, Paris, France. Energy Dispersive X-ray Spectroscopy (EDXS) data were collected at the same electron beam-voltage using a BRUKER AXS Si-drift detector. CaO was neglected as it occurs only in titanite in the selected metasedimentary rocks. Metabasites were modeled in the Mn – Na_2O – K_2O – CaO – FeO – MgO – Al_2O_3 – SiO_2 – H_2O (MnNKFMASH) system. The following solid solution models were used: garnet, and phengite (Holland and Powell, 1998), omphacite (Holland & Powell, 1996), plagioclase (Newton et al. 1980), chloritoid (White et al., 2000), carpholite and chlorite (Holland and Powell, 1998). Amphibole was modelled using the glaucophane-tremolite-tschermakite-pargasite (GITrTsPg) solid-solution model (Wei and Powell 2003; White et al. 2003). Zoisite/clinozoisite was used as a proxy for epidote. In both metasedimentary and metamafic rocks, additional assumptions were made: (i) water was considered in excess due to the abundance of hydrous phases, (ii) all Fe was considered as ferrous because normalized probe data of the studied mineral

Fig. 9. Representative microstructural relationships between the diagnostic HP minerals and deformation. A) Distinct HPP crenulation cleavage on primary stratigraphic compositional layers. These structures are characteristic of the lower-grade eastern part of the BSZ. B) Penetrative Alpine schistosity resulting from the superposition of HPP (in red) and HPr (in white) fabrics in metapelites of the BSZ. C) Microlithon preserving relicts of HPP fabrics defined by chloritoid and phengite in metapelites from the BSZ. Note that the chloritoid crystal is also parallelized to the new forming schistosity. Due to the partial overprint of chloritoid within the foliation, we attributed this fabric to HPr conditions. D) Superposition of HPP and HPr fabrics in a lawsonite-bearing metasedimentary rocks from the BSZ. Note that lawsonite precipitated synkinematically with respect to the first fabric (which is included in lawsonite crystals, HPP), and successively rotated by a second fabric. Owing to the slightly lower Si content in phengite, the latter fabric is referred to HPr conditions. E) LP crenulation cleavage associated with LP upright open folds in metapelites from the BSZ. F, G) Microstructural relationships between HPP and HPr fabrics in garnet-bearing metacherts of the EZ. Note the relicts of HPr fabrics and mineralogy, e.g. garnet and phengite in (F) and blue amphibole in (G) preserved in microlithons. In (G), note that blue amphibole is partially transformed into chlorite during the HPr deformation. H) Relict of HPP lawsonite wrapped around by the HPr schistosity. Lawsonite is partially replaced by paragonite aggregates during this stage, but it still preserves relicts of the HPP fabrics defined by tiny acicular rutile and organic matter.

assemblages reveal little ferric iron and because the solid solutions models for Fe^{3+} -bearing silicates are not very accurate (Ghent et al., 2009), and (iii) CO_2 was neglected due to the occurrence of titanite porphyroblasts, which suggests a low CO_2 activity (Castelli et al., 2007), and lawsonite, which is extremely sensitive to CO_2 (Goto et al., 2007).

6.3. RSCM results

A dense sampling was performed along two representative profiles almost parallel to the main dip of the Alpine foliations and as isolated samples (Figs. 2B, 10, 11), aiming at providing a high-resolution cross-



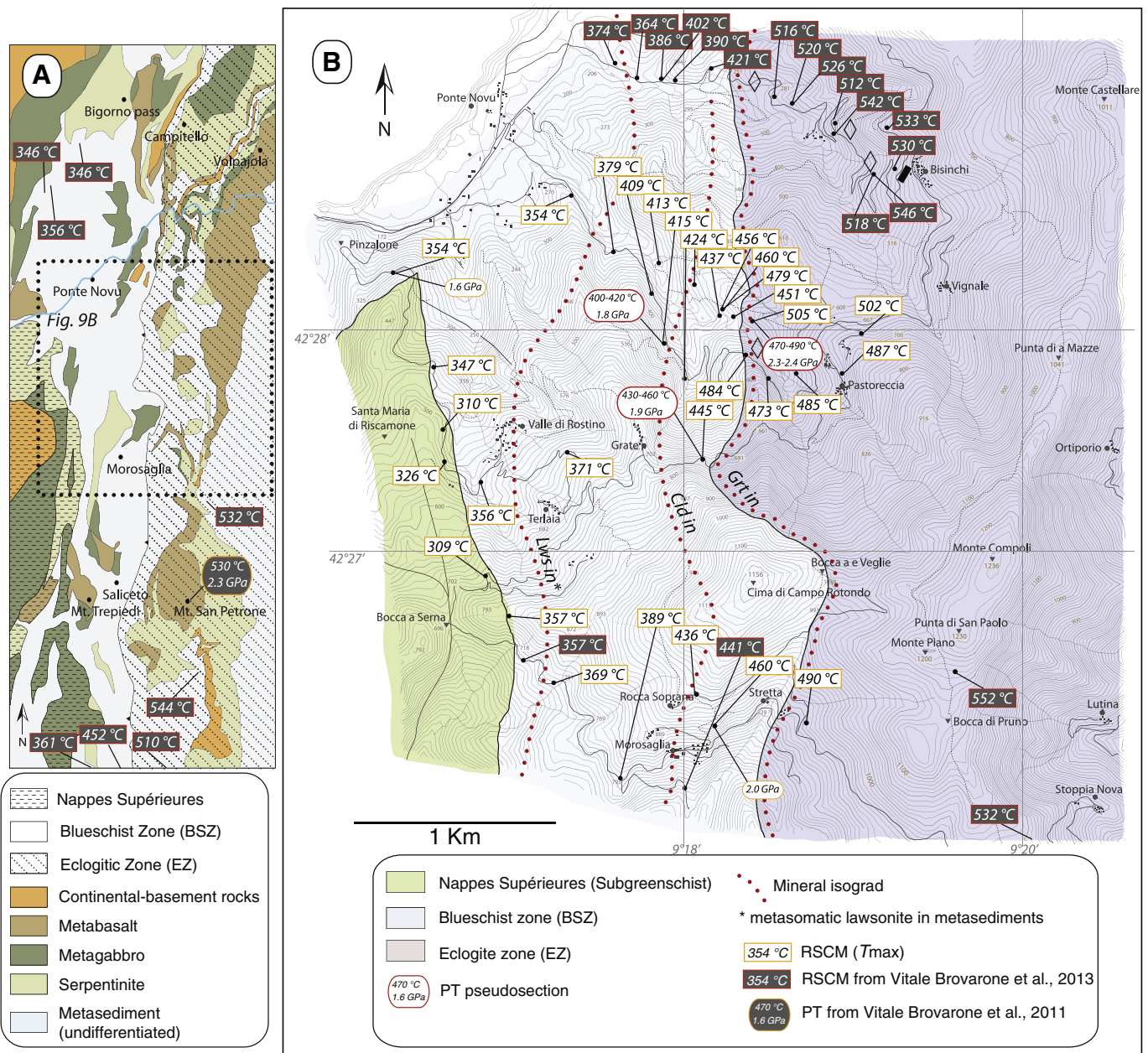


Fig. 10. A, B) Metamorphic map of the studied area showing the RSCM T_{max} and peak P-T estimated via pseudosection modeling. In B, the detected metamorphic mineral isograds are outlined by the dotted curves.

section through the blueschist–eclogite transition compared to the belt-scale dataset provided by Vitale Brovarone et al. (2013). Data are reported in Table 3. Additional data along a third profile passing across the northern part of the study area are available in Vitale Brovarone et al. (2013) and are reported in Fig. 10.

Only two samples belong to the Nappes Supérieures, and yield RSCM-T of 309 and 310 °C (Figs. 10, 11, Table 3). In the BSZ, RSCM-T of ~350 °C characterize the western part, and progressively increases eastward to about 460–480 °C at the contact with the EZ. The only exception is the slightly scattered pattern associated with continent-derived metaconglomerate bodies, which possibly reflects the presence of a detrital CM component. The EZ shows a slight eastward (and down-section) T increase from ~480–490 °C to ~530–550 °C.

The appearance of diagnostic HP minerals in the study area is systematically correlated with discrete RSCM metamorphic T.

The appearance of metasomatic lawsonite in metapelites systematically coincides with RSCM-T of about 360–380 °C (Fig. 10) (see also Vitale Brovarone et al., 2014). Chloritoid in metapelites of the BSZ corresponds to a RSCM-T of 415–440 °C. The appearance of garnet, which corresponds to the BSZ–EZ tectonic boundary, corresponds to a RSCM-T of ~470–490 °C. Note that the appearance of garnet should not be considered as a metamorphic isograd, and likely coincides with a major tectonic discontinuity (see Discussion).

6.4. P–T pseudosections

Samples for pseudosection calculation were selected close to the BSZ–EZ boundary, in both metasedimentary and mafic rocks. In the BSZ, HP assemblages in metasedimentary rocks are well preserved,

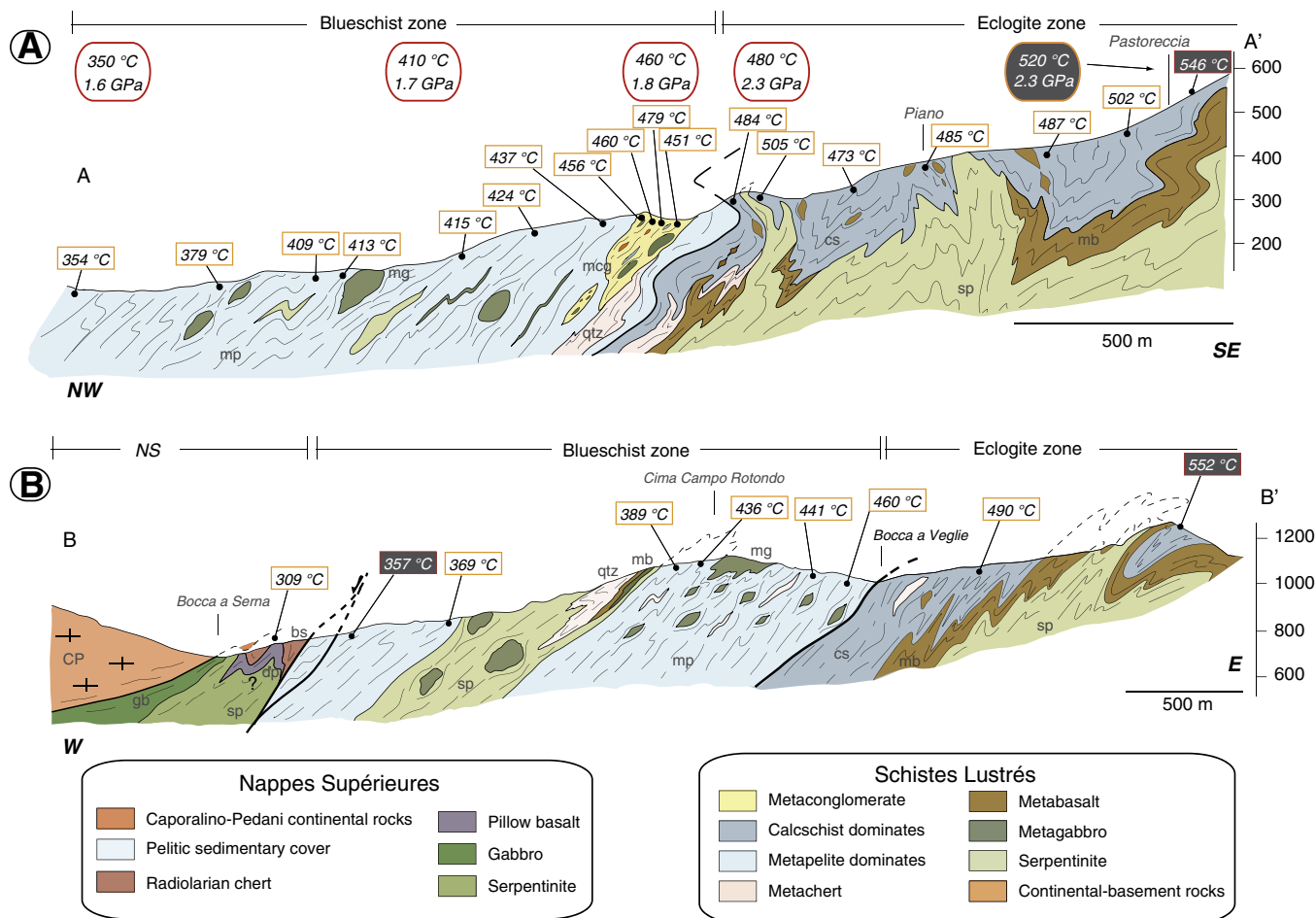


Fig. 11. Geological cross-sections across the mapped area (see Fig. 2A for location of the two profiles and for color codes) showing the estimated P-T condition. Dark boxes refer to P-T estimates by Vitale Brovarone et al. (2011a) and Vitale Brovarone et al. (2013).

whereas metabasites contain amphibole-rich, garnet-free assemblages that are challenging to model. On the contrary, in the EZ, metasedimentary rocks are strongly overprinted and metabasites offer the best chance for P-T estimates. For this reason, we selected fresh metasedimentary and fresh metabasic rocks for P-T estimates in the BSZ and EZ, respectively. All samples were selected close to the contact zone between the two units, in order to evaluate the P gap across the contact. Two samples of chloritoid-bearing metapelite were selected from the BSZ, and mostly consist of phengite, chlorite, quartz, tiny chloritoid crystals and CM. In sample OF3778, which corresponds to the chloritoid-in metamorphic isograd, the celadonite substitution in prograde phengite preserved in microlithons reaches 3.40–3.43 a.p.f.u., and chloritoid X_{Mg} reaches 0.07 (Table 2; Fig. 12A). Phengite (X_{Si}) and chloritoid (X_{Mg}) compositional isopleths constrain HP peak conditions at $T = 400\text{--}420\text{ °C}$ and 1.8 GPa in the quadri-variant field $Chl + Phe + Ctd + q (+H_2O)$ (Fig. 12A). This T value fits well with the RSCM-T estimated for this sample, i.e. $T = 424\text{ °C}$ (Figs. 10, 11; Table 3). Sample OF3745 was collected close to the village of Grate, and shows a slightly higher celadonite substitution in phengite (3.45 a.p.f.u.), and X_{Mg} in chloritoid up to 0.09 (Table 2). P-T conditions are estimated at $T = 430\text{--}460\text{ °C}$ and $P = 1.9\text{ GPa}$ based on phengite (X_{Si}) and chloritoid (X_{Mg}) compositional isopleths (Fig. 12A). The T estimated via pseudosection fits well with the range of RSCM-T for this sample, i.e. 454 °C.

Two samples of metasedimentary rocks lacking chloritoid were selected for qualitative P estimates based on the phengite celadonite content and the associated RSCM-T. Sample OF3698 was collected at the very bottom of the Santa Reparata metaconglomerate. The highest

celadonite substitution reaches 3.45–3.50 (a.p.f.u.), and corresponds to P of about 1.9 GPa for a RSCM-T of 460 °C (Fig. 12A). By means of the same approach, a sample from the western part of the BSZ (sample OF3781, Si in phengite = 3.33–3.37 a.p.f.u) plots at $P = 1.6\text{ GPa}$ for a RSCM-T of 354 °C (Fig. 12A), which are compatible with the occurrence of carpholite. The P-T conditions obtained in the studied chloritoid-bearing samples are compatible with the absence of garnet in the peak assemblages, which are otherwise modeled above ca. 500 °C and 2.0 GPa. These conditions are in turn compatible with the P-T estimates of the EZ, where garnet was found in some metasedimentary samples.

In the EZ, as metasedimentary rocks commonly display intense retrogression, P-T conditions were estimated on a fresh sample of metagabbro. Previous P-T estimates in the highest-grade part of the EZ, where surrounding schists yield RSCM-T of ~530–550 °C, provided $T = 520 \pm 20\text{ °C}$ and 2.2–2.4 GPa (Vitale Brovarone et al., 2011a), and we herein investigate P-T condition close to the boundary with the BSZ, where slightly lower RSCM-T are observed (480–500 °C, Figs. 10, 11). Sample OF3704 is a block of metagabbro enclosed in a metasedimentary matrix from the highly sheared contact separating the BSZ and the EZ, and consists of two coexisting amphiboles (glaucophane and actinolite, respectively, Tables 1, 2), lawsonite, garnet, phengite, chlorite, apatite, quartz and titanite. This particular paragenesis is common in lawsonite–eclogite-facies metamafics of Alpine Corsica, and does not show significant retrogression aside from local late chlorite overprinting garnet and glaucophane. Note that the absence of omphacite in this sample does not reflect retrogression but is due to a X_{Ca} -poor bulk-rock composition (cf. Vitale Brovarone et al., 2011a for details). Relicts of a former Ca-rich glaucophane generation

Table 3
Selected samples for RSCM thermometry. GPS coordinates in WGS84 system, number of spectra (n), mean R2 ratio (Beysac et al., 2002) or RA1 ratio (Lahfid et al., 2010) for n spectra with corresponding standard deviation (sdv), and calculated temperature with standard error (SE). Standard error is the standard deviation divided by Vn. The absolute error on temperature is ± 50 °C [Beysac et al., 2002].

Sample	Locality	Lat	Long	n.	R2/RA1*	SD	T (°C)	SE
OF3689	Castello di Rostino	42° 28' 1.42"	9° 18' 20.37"	13	0.31	0.03	505	4
OF3691	Stretta	42° 26' 10.07"	9° 18' 39.70"	12	0.34	0.02	490	3
OF3693	Pastoreccia	42° 27' 50.28"	9° 18' 53.24"	14	0.35	0.05	487	6
OF3695	Castello di Rostino	42° 28' 36.54"	9° 17' 17.52"	13	0.65	0.03	354	4
OF3698	Morosaglia	42° 26' 12.55"	9° 18' 9.47"	12	0.41	0.03	460	4
OF3701	Rocca Soprana	42° 26' 21.65"	9° 17' 59.18"	7	0.46	0.06	436	10
OF3724	Valle di Rostino	42° 27' 24.76"	9° 17' 07.53"	13	0.61	0.04	371	5
OF3725*	Valle di Rostino	42° 27' 25.54"	9° 16' 29.99"	12	0.64	0.01	326	2
OF3733*	Bocca a Serna	42° 26' 53.97"	9° 16' 45.09"	13	0.62	0.01	309	3
OF3736	Castello di Rostino	42° 28' 2.97"	9° 18' 12.41"	23	0.42	0.03	456	3
OF3737	Castello di Rostino	42° 28' 2.97"	9° 18' 12.41"	23	0.36	0.05	479	5
OF3738	Castello di Rostino	42° 28' 2.97"	9° 18' 12.41"	23	0.41	0.07	460	6
OF3741	Castello di Rostino	42° 28' 19.00"	9° 17' 46.77"	15	0.5	0.02	413	2
OF3746	E-Grate	42° 27' 24.32"	9° 18' 3.20"	14	0.44	0.03	445	4
OF3748	Castello di Rostino	42° 27' 56.64"	9° 17' 50.79"	14	0.51	0.02	415	3
OF3754	Piano	42° 27' 49.35"	9° 18' 37.74"	13	0.35	0.04	485	5
OF3755	Castello di Rostino	42° 28' 4.46"	9° 18' 11.19"	20	0.46	0.04	437	4
OF3766	W-Castello di Rostino	42° 28' 22.33"	9° 17' 30.98"	15	0.59	0.02	379	3
OF3772	E-Castello di Rostino	42° 27' 58.69"	9° 19' 1.74"	16	0.31	0.05	502	5
OF3775	Castello di Rostino	42° 27' 47.75"	9° 18' 28.01"	15	0.37	0.04	473	5
OF3778	Castello di Rostino	42° 27' 47.18"	9° 17' 58.93"	20	0.49	0.03	424	3
OF3780	Castello di Rostino	42° 28' 9.81"	9° 17' 46.56"	20	0.52	0.02	409	2
OF3781	E-Pinzalone	42° 28' 16.83"	9° 16' 10.16"	15	0.64	0.01	354	1
OF3783	W-Valle di Rostino	42° 27' 52.51"	9° 16' 22.67"	14	0.66	0.01	347	1
OF3786	Valle di Rostino	42° 27' 19.59"	9° 16' 41.61"	14	0.64	0.01	356	1
OF3788	Bocca a Serna	42° 26' 42.93"	9° 16' 51.04"	14	0.64	0.01	357	1
OF3792	S-Valle di Rostino	42° 27' 20.39"	9° 16' 58.03"	14	0.59	0.02	375	2
OF3794*	W-Valle di Rostino	42° 27' 33.63"	9° 16' 30.38"	12	0.62	0.01	310	3
OF3797	E-Bocca a Serna	42° 26' 24.57"	9° 17' 9.12"	20	0.61	0.03	369	3
OF3805	E-Castello di Rostino	42° 28' 1.05"	9° 19' 26.45"	13	0.13	0.07	581	9
OF3811	Castello di Rostino	42° 27' 54.13"	9° 18' 19.85"	16	0.36	0.05	484	6

* Low-T samples processed with RA1 ratio.

(Table 2) core larger amphibole crystals and testify for incomplete peak re-equilibration. Lawsonite forms fine-grained aggregates replacing the igneous plagioclase sites. Garnet forms millimeter blasts characterized by a prograde, bell-shaped Mn compositional zoning and particular optical anisotropy (cf. Vitale Brovarone and Herwartz, 2013 for details and compositional profiles). Phengite shows very high Si content up to 3.6 (a.p.f.u., Table 2). A first generation of chlorite is texturally in equilibrium with garnet, whereas a second one occurs as pseudomorphic product after garnet and glaucophane. Garnet compositional isopleths constrain equilibrium conditions at 470–490 °C and 2.3–2.4 GPa, at the boundary between the di-variant field $\text{Chl} + \text{Omp} + \text{Gln} + \text{Act} + \text{Gt} + \text{Phe} + \text{Law} + \text{q}$ and the tri-variant field $\text{Omp} + \text{Gln} + \text{Act} + \text{Gt} + \text{Phe} + \text{Law} + \text{q}$ (Fig. 12B). Omphacite was not observed in the studied sample, but occurs in negligible amount in the modeled pseudosection (<5 vol.%), and likely depends on the complexity in modeling amphibole-rich equilibria or on the effect of partially re-equilibrated domains (see above). The sample contains chlorite, as modeled in the di-variant field $\text{Omp} + \text{Amp1} + \text{Amp2} + \text{Phe} + \text{Chl} + \text{Gt} + \text{Law} + \text{Q}$ (Fig. 12B). The obtained T estimates fit well with the RSCM-T in the host calcschist (ca. 480–500 °C, Fig. 10B, 12B).

7. Discussion: the blueschist–eclogite transition in the Schistes Lustrés

7.1. Oceanic vs. orogenic origin for the lithological suites

The origin of the lithological associations in HP terranes has been matter of long-standing debates. On one side, the “subduction channel” model ascribes a major role to intense tectonic disruption and “mélange” at the plate interface, including profound mixing between slab- and mantle wedge-derived material (e.g. Blanco-Quintero et al., 2010; Cloos and Shreve, 1988; Guillot et al., 2009; Malatesta et al., 2011). On the other hand, lithostratigraphic observations in poorly

deformed terranes led some authors to interpret a large variety of lithological associations as primary and consistent pieces of subducting lithosphere, often preserving rather undisturbed sequences (see extensive literature by, e.g. Lemoine et al., Lagabrielle et al. and references therein). In the case of units displaying large and rather coherent lithostratigraphic suites, most authors agree with a limited extent of late tectonic mixing (see e.g. Monviso, Lombardo et al., 1978; Corsica: Lahondère, 1996; Meresse et al., 2012; Vitale Brovarone et al., 2011b and references therein). Despite local intense deformation, this type of terrane shows consistent lithological associations, among which the most common is the succession of ophiolitic basement rocks overlain by quartzites, marbles, pelites; or the more recent reevaluation of continental basement slivers sandwiched between serpentinites and metasedimentary rocks as continental extensional allochthons (Beltrando et al., 2014). These configurations are common in the EZ and also locally characterize the lithological associations of the BSZ (see Section 3). Importantly, no evidence of mantle wedge-derived material has ever been found in both units.

On the contrary, due to the more chaotic structure, the interpretation of block-in-matrix structures as either “subduction mélanges” or deformed olistostromes is “the crux of these difficulties” (Wakabayashi, 2012). Block-in-matrix structures were found in both the BSZ and the EZ, but they show striking differences. In the EZ, mafic blocks in a metasedimentary matrix are localized close to the contact with the BSZ, they are intensely internally deformed, and commonly arrayed within the main Alpine schistosity. These characteristics led us to favor the hypothesis of intense Alpine boudinage, but within a coherent unit and without mixing with “exotic” material. In the BSZ, however, ophiolitic material within metasedimentary rocks is widespread and ranges from thin beds to large blocks. Among the several characteristic features of these rocks, two are especially worth underlining: the frequent occurrence of rather undeformed breccias/conglomerates, and the occurrence of

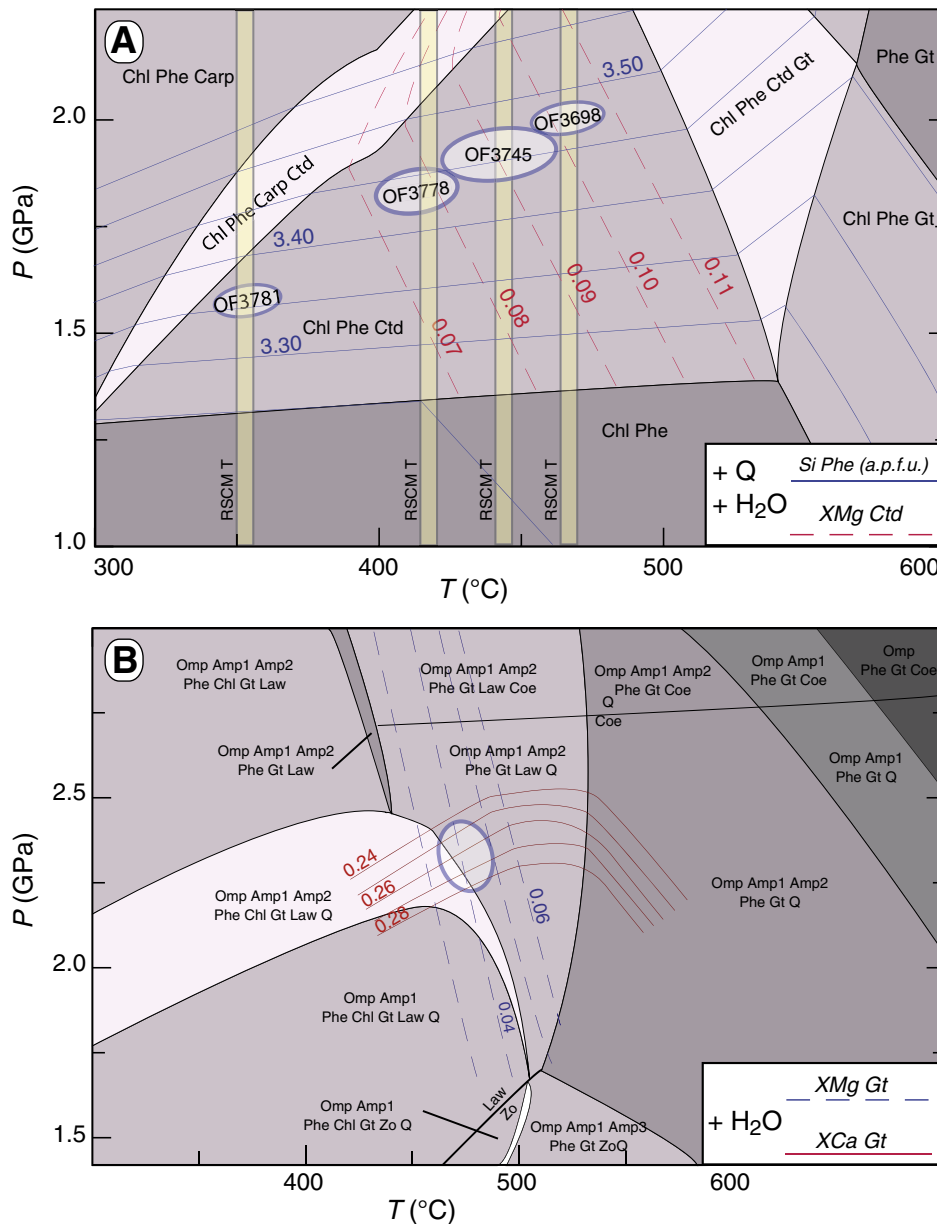


Fig. 12. P–T pseudosection of selected samples of the BSZ metasedimentary samples (A) and the EZ metamafics (B). The modeled bulk rock composition (wt.%) for (A) is $\text{SiO}_2 = 60$; $\text{Al}_2\text{O}_3 = 30$; $\text{FeO} = 3.5$; $\text{MgO} = 3.5$; $\text{K}_2\text{O} = 3$, and for (B) is $\text{SiO}_2 = 53$, $\text{Al}_2\text{O}_3 = 14$; $\text{FeO} = 13$; $\text{MnO} = 0.4$; $\text{MgO} = 7.5$; $\text{CaO} = 9$; $\text{Na}_2\text{O} = 3$; $\text{K}_2\text{O} = 0.1$. In (B), note that all P–T conditions were plotted on the pseudosection calculated for sample OF3745, but each one was estimated on the respective pseudosections. Chl: chlorite; Phe: phengite; Carp: Carpholite; Ctd: chloritoid; Gt: garnet; Q: quartz; Omp: omphacite; Amp1: Na-rich amphibole; Amp2: Ca-rich amphibole; Amp3: Na–Ca amphibole; Law: lawsonite; coe: coesite; Zo: zoisite.

organic matter and carbonates inside the mafic layers/blocks. These features clearly indicate sedimentary mechanism of emplacement of ophiolitic material within metasedimentary rocks. Large blocks of metagabbro are therefore interpreted as olistostromal bodies, following the conclusion of previous works in the Western Alps analogues of these units (e.g. Deville et al., 1992; Lagabrielle, 1987; Lagabrielle and Cannat, 1990; Lagabrielle and Polino, 1985; Le Mer et al., 1986; Lemoine, 1980; Lemoine et al., 1987; Tricart et al., 1982). The availability of exposed gabbros and serpentinites at the seafloor as sources for ophiolitic olistostromal deposits is a characteristic feature of slow-spreading oceans like the Atlantic Ocean and the Alpine Tethys (Lagabrielle and Cannat, 1990; Sauter et al., 2013). These surfaces, and their contact with the overlying sedimentary cover sequence, are locally preserved in the studied units, and locally marked by diagnostic rock types such as ophicarbonates (e.g. Fig. 3A, B).

7.2. Contrasted lithostratigraphic patterns between EZ and BSZ

The blueschist–eclogite transition in the Schistes Lustrés of Alpine Corsica is associated with an abrupt lithological contrast. The BSZ comprises mainly metapelites and marble layers with volumetrically minor serpentinites/gabbro-dominated metaophiolites, intercalated at various levels within the metasedimentary sequence. Alternatively, the EZ is characterized by prevailing metaophiolites, mostly consisting of serpentinites and metabasalts, and associated calcschists. Our field observations permit the primary stratigraphic relationships among the different lithologies to be locally established. The resulting tectonostratigraphic suites are summarized in Fig. 13 and described as follows for their major features.

At a closer look, apart from the occurrence of dominant metasedimentary rocks in the BSZ and dominant metaophiolites in the EZ, the two units show subtle but important tectonostratigraphic

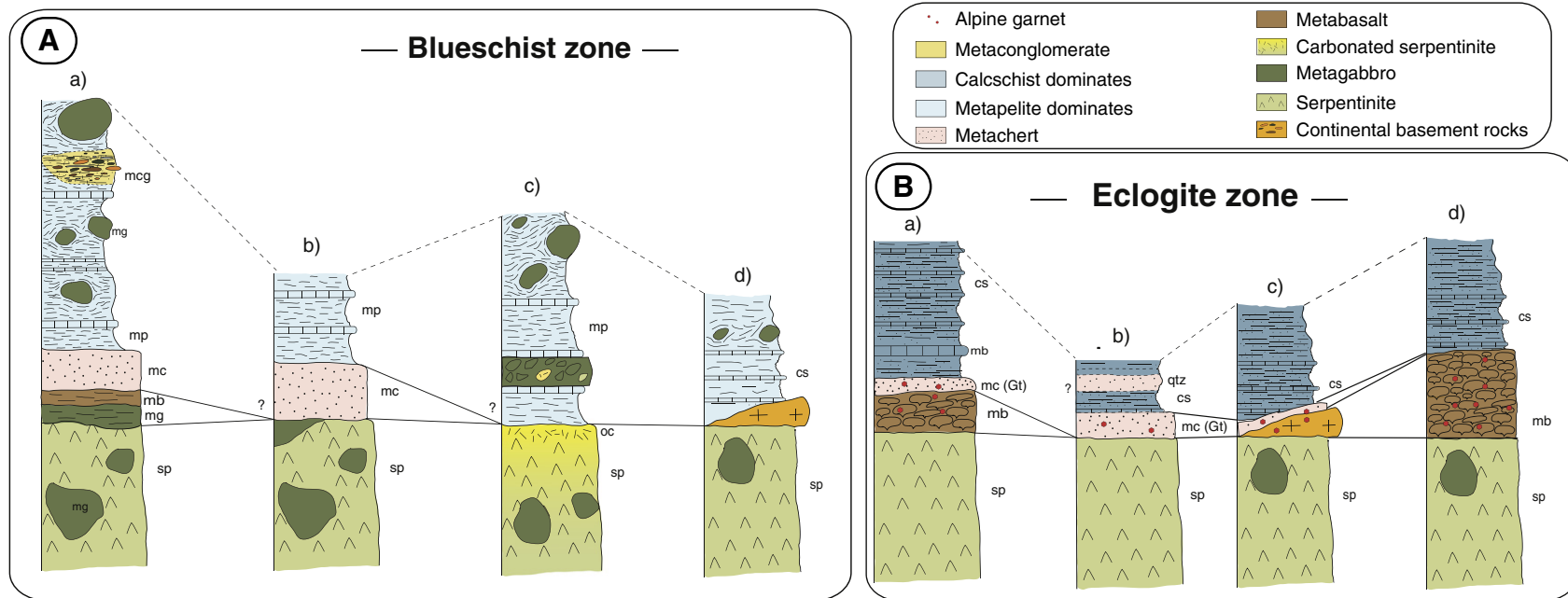


Fig. 13. Reconstructed tectonostratigraphic logs of the BSZ (A) and the EZ (B). A) a, b) Monte Campo Rotondo area (Fig. 2B). In (a), the Santa Reparata metaconglomerate is put in the upper part of the log; however, field analyses did not permit to clarify the primary structural position, and a deeper structural position is not excluded. c) Bigorno pass area (Fig. 2A). Note the occurrence of ophicarbonate, likely carbonated serpentinites, atop of the ultramafic basement, and of ophicarbonate clasts within gabbroic metabreccias. d) Campitello area. In this case, the serpentinitized basement is overlain by a slice of continental basement rocks interpreted as a Tethyan extensional allochthons (Meresse et al., 2012; Vitale Brovarone et al., 2011b). This continental basement sliver is also locally found further to the north, close to the Rutali village, in the Cima Zuccarello and Serra di Pigno areas. B) a) Castello di Rostino ridge. b) Frasso area. Note the occurrence of garnet in metachert (dots) in both a) and b). c) Bocca di Pruno area. Also in this case, as log d in the BSZ, small continental extensional allochthons are locally found atop the ultramafic basement. In the EZ, other slices are found in the San Petrone area (Vitale Brovarone et al., 2011b) d) Monte Compoli area. sp: serpentinite. mg: metagabbro. mb: metabasalt. mc: metachert. mp: metapelite. mcg: metaconglomerate. oc: ophicarbonate. cs: calcschists.

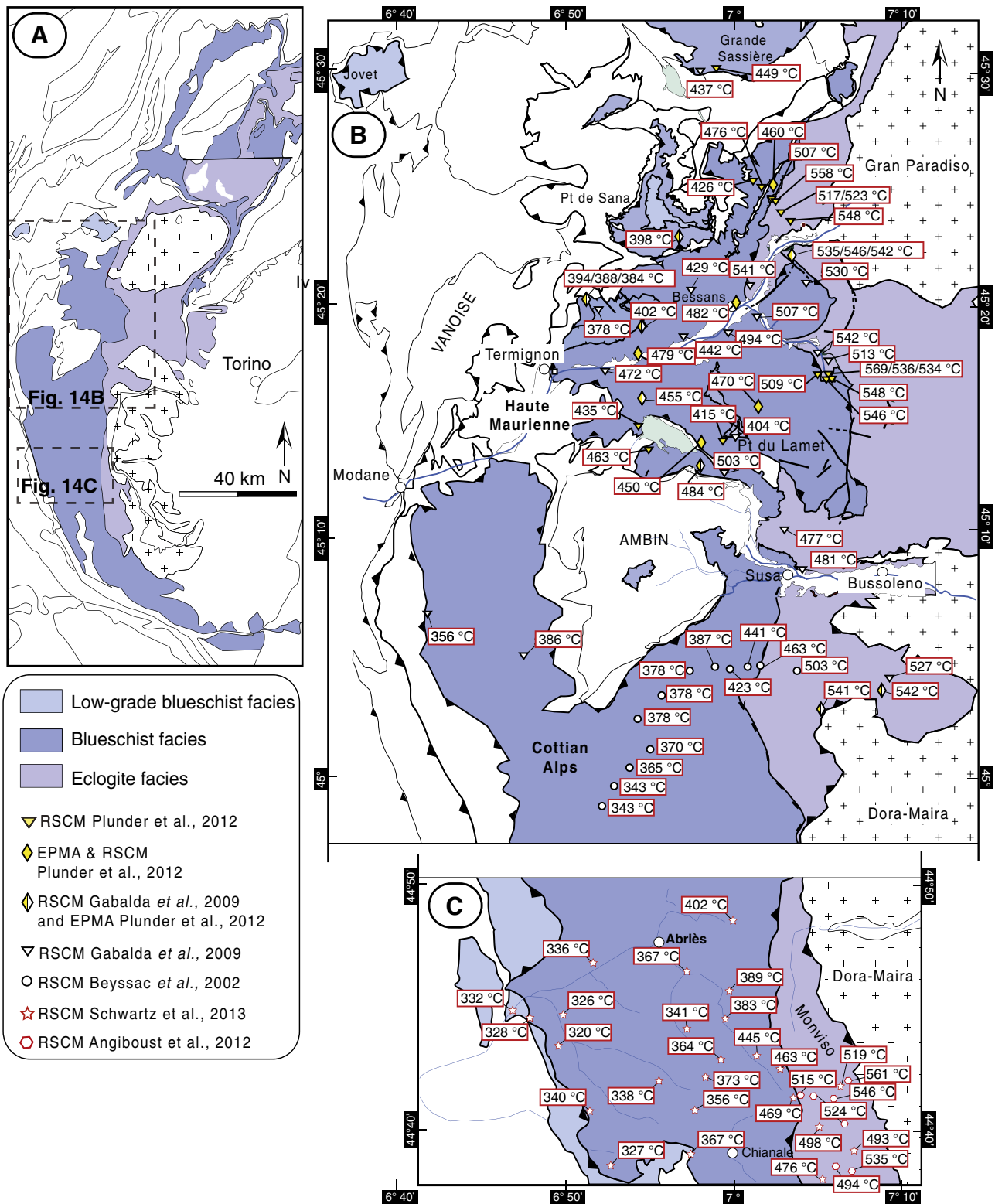


Fig. 14. Metamorphic maps of the Schistes Lustrés units of the Western Alps. A. Modified after Beltrando *et al.*, 2010b. B, C. Details of the blueschist–eclogite transition in the Piemonte Zone of the Western Alps showing the published RSCM dataset across the blueschist–eclogite transition. In B, data from Beyssac *et al.* (2002), Gabalda *et al.* (2009) and Plunder *et al.* (2012). Modified after Plunder *et al.* (2012). In C, data from Schwartz *et al.* (2012) and Angiboust *et al.* (2011).

differences (Fig. 13). Both units show typical supraophiolitic sedimentary sequences, such as metacherts, metalimestones, to more pelitic material upwards, but, notably, metapelites and calcschists prevail in the BSZ and in the EZ, respectively. The BSZ is characterized by remnants of denudated ultramafics, often containing abundant gabbroic bodies,

and the common occurrence of gabbro-dominated ophiolitic debris and olistostromes intercalated within a mostly pelitic sedimentary sequence (Fig. 13A). Metavolcanics are rare and form localized bodies. Similar settings have been extensively documented in the Queyras region of Western Alps and have been already compared to the Inzecca

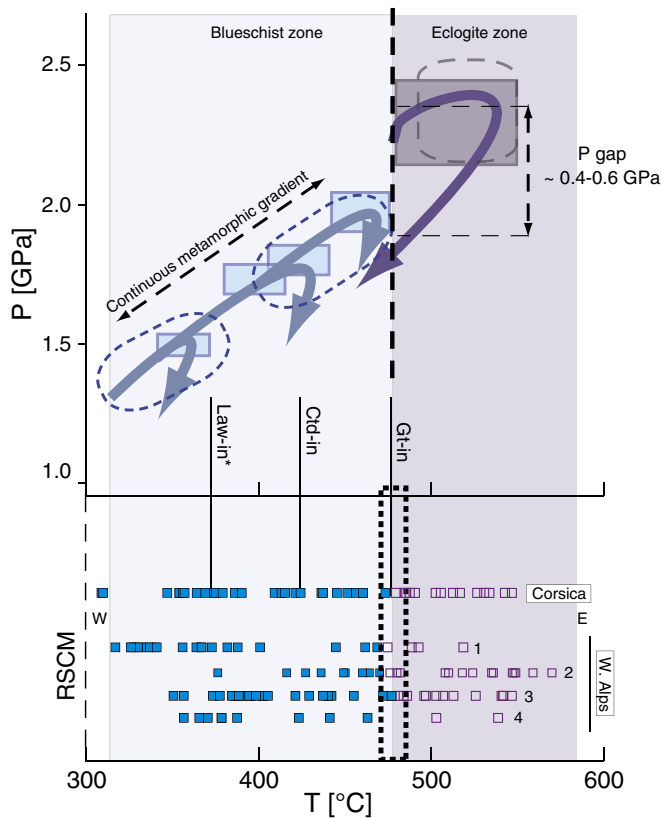


Fig. 15. P–T diagram showing the metamorphic climax estimates in the studied area (squares), together with those estimated in the Western Alps (ellipses). Metamorphic conditions for Corsica from this study and Vitale Brovarone et al. (2011a); for the Western Alps by Beyssac et al. (2002); Gabalda et al. (2009); Angiboust et al. (2009, 2011); Groppo and Castelli (2010); Plunder et al. (2012); Schwartz et al. (2012). RSCM data from: 1: this study; 2: Schwartz et al. (2012); 3: Plunder et al. (2012); 4: Gabalda et al. (2009); 5: Beyssac et al. (2002). *The lawsonite-in isograd refers to the appearance of metasomatic lawsonite in metasedimentary rocks.

Formation of Corsica and the less deformed units of the Apennines (Lagabriele and Cannat, 1990; Lagabriele and Lemoine, 1997; Lemoine, 2003; Lemoine et al., 1987; Tricart, 1974).

In the BSZ, the amount of continental material increases progressively toward the contact with the EZ: i) it is absent in the lowest-grade condition (low-grade blueschist unit in Vitale Brovarone et al., 2013, cf. Section 2), ii) it occurs as small conglomeratic lenses in the highest-grade part of the BSZ (Lawsonite–blueschist unit in Vitale Brovarone et al., 2013) and as continental basement slivers toward the contact with the EZ (e.g. Caron and Delcey, 1979; Lahondère, 1996; Meresse et al., 2012; Vitale Brovarone et al., 2011b). These features suggest a progressive transition from more distal to more proximal (OCT) origin moving upward in the tectonic pile (and from the highest to the lowest metamorphic grade). Continent-derived debris also exists within the blueschist-facies metapelites of some units of the Western Alps, and testifies for a comparable paleogeographic origin, close to a continental margin (Caby et al., 1971; Polino and Lemoine, 1984).

The EZ is characterized not only by a thicker metaophiolitic basement, mostly consisting of serpentinites and metabasalts (Fig. 13B), but also shows a thick metasedimentary cover sequence of prevailing calcschists. Reworking of mafic/ultramafic is common within the ophiolitic pile (e.g. the so-called Mandriale unit, cf. Vitale Brovarone et al., 2013), but ophiolitic breccias within metasedimentary series are rare compared to the BSZ. Also in the EZ, the frequent occurrence of continental basement material suggests an OCT origin (e.g. Vitale Brovarone et al., 2011b). The eclogite-facies unit of the Schistes Lustrés of the Western Alps, such as the Monviso or Zermatt–Saas units shows comparable tectonostratigraphic features, with dominant metavolcanics

(Lagabriele and Lemoine, 1997; Lombardo et al., 1978, 2002) and local continental extensional allochthons (Beltrando et al., 2010a). The sedimentary cover of the Monviso unit does not show the typical Ligurian succession of oceanic affinity, rather it is rich in continent-derived siliciclastic material (Baracun Formation, Lagabriele, 1994).

7.3. Contrasted metamorphic patterns

The second striking difference between the BSZ and EZ is the Alpine metamorphism, as outlined by mineral isograds, RSCM thermometry and P–T pseudosections. RSCM thermometry provides the maximum T experienced by CM bearing rocks, independently from retrogression. In the case of Alpine Corsica, the preservation of HP–LT phases such as lawsonite suggests a cold retrograde path, and the absence of significant decompressional heating. This feature permits to ascribe both T_{\max} by RSCM and P_{\max} estimated by pseudosection modeling to the same metamorphic event. The good fit between RSCM T_{\max} and T associated with P_{\max} estimated via pseudosection modeling corroborate this assumption.

In the BSZ, metamorphic conditions increase progressively from lower-grade ($P = 1.5\text{--}1.6$ GPa at $T = 350$ °C) to higher-grade ($P = 1.8$ GPa at $T = 460\text{--}480$ °C) lawsonite blueschist-facies conditions, without significant metamorphic gaps. Metamorphic mineral isograds (i.e. lawsonite–chloritoid) are homogeneously distributed over the studied area and correspond to specific metamorphic conditions (Figs. 10 and 11). In the Western Alps, the blueschist-facies, metasediment-rich zone (Queyras, Combin) shows the same progressive increase of metamorphism, from ca. 330–350 °C/0.7–1.1 GPa to ca. 470–480 °C/1.8 GPa (Beyssac et al., 2002; Gabalda et al., 2009; Plunder et al., 2012; Schwartz et al., 2012) (Fig. 14), and comparable mineralogical patterns (Plunder, 2013, pers. com.). The only difference between the two belts is the occurrence, in the Western Alps, of an epidote–blueschist zone, which is not observed in Corsica. However, this feature can be related to the effect of a much more pervasive retrograde overprint in the Western Alps, as recently proposed for similar metamorphic trends in the blueschist terranes of New Caledonia (Vitale Brovarone and Agard, 2013). This latter hypothesis is supported by the estimated peak P–T conditions for BSZ rocks, which plot in the lawsonite stability field, as for the Western Alps (Fig. 12).

The EZ is characterized by lawsonite–eclogite-facies assemblages. Also in this zone, a slight eastward T gradient is observed, from 470–490 °C to ca. 530–550 °C, but P estimates are rather constant and points to ca. 2.3–2.4 GPa (Fig. 11; Vitale Brovarone et al., 2011a). The eclogite-facies, metaophiolite-rich units of the Western Alps show, again, similar P–T estimates at ca. 480 to 550 °C, and 2.2–2.6 GPa (Angiboust et al., 2009, 2011; Beyssac et al., 2002; Gabalda et al., 2009; Groppo and Castelli, 2010; Plunder et al., 2012; Schwartz et al., 2012) (Figs. 14 and 15).

7.4. Metamorphism and deformation across the blueschist–eclogite contact zone

The P–T patterns across the blueschist–eclogite boundary of the two belts require a careful discussion. The P gap observed in our study in Corsica and, by compilation, in the Western Alps suggests the occurrence of a tectonic gap between the blueschist-facies and the eclogite-facies terranes. Despite the fact that no significant T gap is observed across this contact, which might suggest a limited displacement, petrologic arguments indicate the occurrence of a considerable tectonic elision along the blueschist–eclogite boundary. The main argument for that is the sudden appearance of eclogite-facies minerals along this contact, which is unlikely in the case of a continuous metamorphic gradient. As an example, the appearance of garnet in metabasic and metasedimentary rocks is sharp and not attenuated with lithological compositions more or less favorable to garnet formation (e.g. Mn-rich/poor rocks). Moreover, omphacite in the BSZ is limited to veins or occurs in little amount in mafic rocks, whereas it is a common and abundant

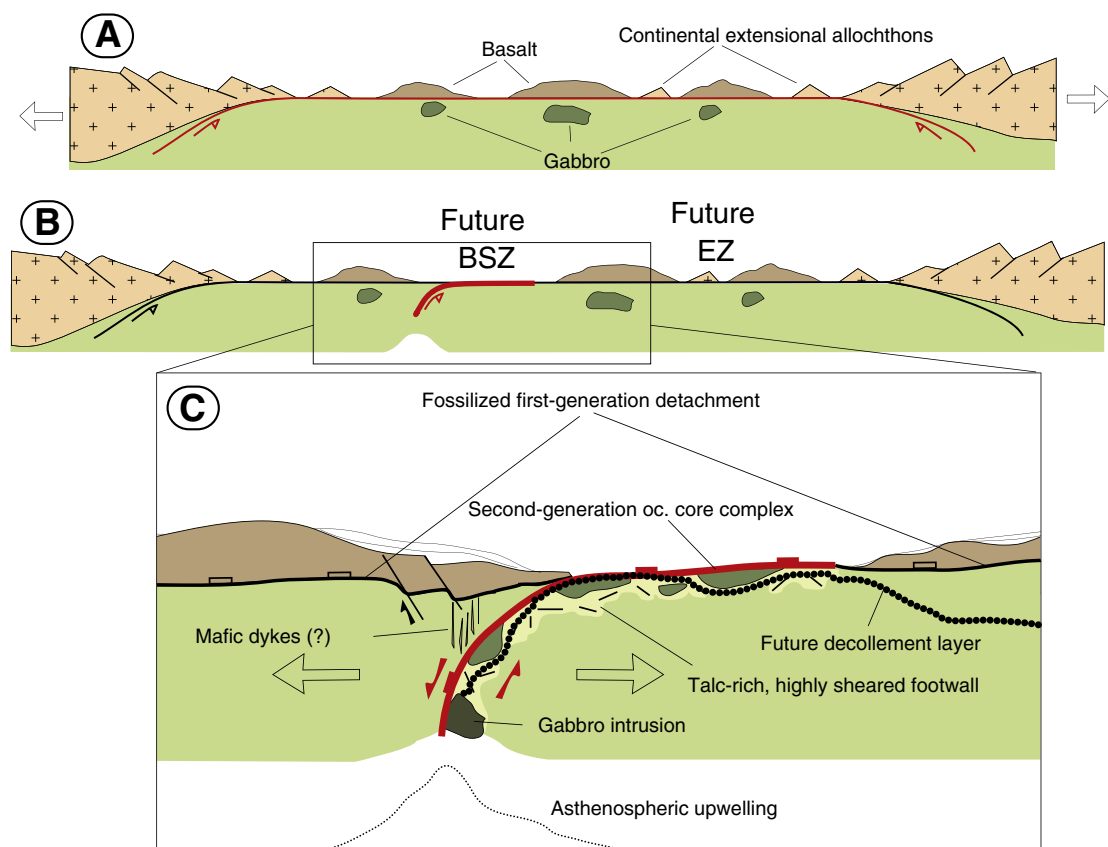


Fig. 16. Idealized genetic model of the BSZ and EZ terranes. In A, mantle rocks are exhumed by means of a first generation of low-angle detachment faults followed by a first magmatic stage. In B and C (close up), a second generation of low-angle extensional structures exhumes new ultramafic substratum and the associate, newly formed gabbroic rock. The second-generation core complex is associated with asthenospheric upwelling (C). Note the abundance of gabbroic rock and talc-rich shear zones in the footwall. The oceanic core complex geometry in C is modified after [Cannat et al. \(2009\)](#). The future decollement layer during subduction in the two types of crust is highlighted by the dotted line. The geometry proposed in this model also considers the occurrence of different sedimentary cover sequences in the BSZ and the EZ, possibly due to diachronous exposure at seafloor, and the progressive increase of continent-derived material moving downward from the gabbro-rich, lower-grade BSZ, to the basalt-rich EZ.

component of several rock types throughout the EZ. These patterns are unlikely in the case of a progressive increase of metamorphism, and support the hypothesis of a true P gap, as suggested by our estimates pointing to a gap of ca. 0.2–0.6 GPa ([Fig. 12](#)). Importantly, the same P gap was estimated by means of different techniques by [Ballèvre and Merle \(1993\)](#) in the Western Alps. For the above reasons, we are confident that our petrographic observations and petrologic estimates reflect a real P gap between the two units. Interestingly, a similar P gap also separates the metasediment-rich blueschist terranes from the metaophiolite-rich eclogite terranes of New Caledonia ([Vitale Brovarone and Agard, 2013](#)).

Maximum T estimated by means of RSCM show a progressive increase of metamorphism across this contact, and no T gap is observed. This pattern has been observed by several authors in the Western Alps and across different profiles ([Beyssac et al., 2002](#); [Gabalda et al., 2009](#); [Plunder et al., 2012](#); [Schwartz et al. 2012](#); [Figs. 11 and 12](#)), and therefore cannot be considered as a local feature. In the two belts, eclogite-facies assemblages occur starting from the restricted T range of 470–490 °C ([Figs. 10, 11, 14 and 15](#)). This feature is again unlikely in the case of late tectonic discontinuities (e.g. late extensional faults), which would have more scattered patterns. In the Western Alps, the contact separating the two units (blueschist- and eclogite-facies) has been interpreted as a late, greenschist-facies extensional fault ([Ballèvre and Merle, 1993](#); [Ballèvre and Merle, 1990](#)). However, in Corsica, several field arguments suggest an early origin for this contact. In the BSZ, lawsonite, which is an HP phase extremely sensible to retrograde overprint, is well preserved in the proximity of the contact with the EZ, thus constraining the motion along this contact to lawsonite-in, HP conditions. Furthermore, this contact is folded by LP recumbent folds (cf. [Section 5](#)), indicating at least

pre-LP deformation juxtaposition. We therefore propose that this contact originated at depth during the exhumation of the EZ to blueschist-facies conditions, and was only lately reactivated during uplift at greenschist-facies conditions (see also the polyphased evolution proposed by [Ballèvre and Merle, 1993](#) for the Combin Fault in the Western Alps).

Data from Corsica and the Western Alps suggest that the P–T path across the blueschist–eclogite transition is characterized by a steep, rather isothermal increase of pressure corresponding to a T of ca. 480–500 °C ([Fig. 15](#)).

The occurrence of lower-grade units beneath the EZ, i.e., the Castagniccia unit (see [Vitale Brovarone et al., 2013](#)), may be seen as a limitation of our model. However, the Castagniccia terranes have been referred to a continental margin, and thus do not represent part of an oceanic (or transitional) oceanic subduction. From a geodynamic point of view, the Castagniccia units may represent an equivalent of the internal crystalline massifs of the Western Alps (Dora Maira, Gran Paradiso, Monte Rosa), and their lower grade compared to the overlying EZ can be explained by the embryonic collisional evolution experienced in Corsica compared to the Western Alps.

The observed P gap in absence of relevant T gap appears to be a suitable configuration for the possible effect of tectonic overpressure. This mechanism has been shown to require rheological (or lithological) contrast in order to develop (e.g. [Mancktelow, 2008](#)). However, the boundary separating the two units, i.e. BSZ and EZ, only locally corresponds to a lithological contrast (e.g. metasedimentary rocks vs. metabasalt), and most commonly occurs within rather comparable metasedimentary rocks. For this reason, at a first approximation, the contribution of tectonic overpressure is probably negligible in this case.

7.5. Contrasted styles of accretion during shortening

The BSZ and EZ of Alpine Corsica exhibit different deformation patterns. In the BSZ, field observations suggest the tight repetition of small, metasediment-rich slices locally floored by metaophiolites. In contrast, the ophiolitic rocks of the EZ form a rather large and continuous sheet. In the EZ, metamorphism slightly increases from ca. 490 to 550 °C, at a constant P of ca. 2.3 GPa. In the BSZ, the T gradient of 350–480 °C occurs across a structural thickness of 1.5 km, and also corresponds to a gradual P increase, i.e. 0.5 GPa from the lower- and upper-grade part of the BSZ. This very condensed metamorphic gradient implies a factor of attenuation of ca. 15 during exhumation (calculated considering a differential burial of ca. 0.5 GPa and an average dip in the range of 50°) that was likely accommodated by significant penetrative strain, or a combination of penetrative strain and many small extensional faults. This tectonic attenuation is extremely high and we are not aware of any analogues. The T gradient of the EZ is otherwise associated with a rather constant P value (ca. 2.2–2.5 GPa), thus requiring a limited attenuation during exhumation. The timing of this tectonic attenuation in the two units, most notably in the BSZ, clearly post-dates the HP metamorphic climax. An alternative mechanism is proposed in Section 7.6.2.

7.6. Linking oceanic geometries and the tectonometamorphic evolution of Alpine belts

7.6.1. Comparison between fossil and present-day structures of slow-spreading oceans

Detailed lithostratigraphic fingerprints indicate that the blueschist- and eclogite-facies terranes of the Schistes Lustrés of Alpine Corsica and Western Alps sample different types of Tethyan lithosphere, characterized by dominant serpentinites and metagabbro on one hand and by volcanic-rich suites on the other hand (cf. Sections 3 and 7.1). The evidence for large exposures of ultramafics at the seafloor by means of low-angle detachment faults is common in both the BSZ and the EZ, and represents a common feature of both slow-spreading oceans and distal passive margins as well as OCT (Cannat et al., 2009; Lagabrielle, 2009; Manatschal and Müntener, 2009). Along the axis of active slow-spreading ridges, such as the Mid-Atlantic Ridge and the Southwest

Indian Ridge, successive generation of extensional structures lead to the construction of distinct lithological associations (Cannat et al., 2009; Picazo et al., 2012; Sauter et al., 2013; Smith et al., 2008). Serpentine-floored, gabbro-rich zones are abundant in the footwall of large, oceanic core complexes lacking intense volcanic or subvolcanic activity, and where intense reworking of ophiolitic basement rocks also occurs (Sauter et al., 2013). In addition the gabbro-rich footwalls are also characterized by a thick network of talc-rich shear zones (e.g. Picazo et al., 2012), whose possible role during subduction and exhumation is discussed in the next section. Hanging walls of these structures may be otherwise richer in volcanic products that may be generated prior or during the activity of a new detachment fault. This suggests the possible occurrence, in the Alpine Tethys, of two main generations of extensional structures, the first being possibly responsible for the exhumation of mantle rocks in a large OCT zone (now preserved in the EZ, cf. e.g. Lavier and Manatschal, 2006; Lemoine et al., 1987 for early model) whereas the second being responsible for the “oceanization” of a more distal domain (now preserved in the BSZ).

Our tentative model is schematized in Fig. 16 and represents a possible configuration for the fossil Tethyan rocks of the BSZ and EZ in the Schistes Lustrés of Corsica and the Western Alps. In addition, this model may explain the different types of sedimentary covers observed in the two terranes of the Schistes Lustrés, i.e. metapelites in BSZ vs. calcschists in EZ, possibly resulting from the diachronous exposure of basement rocks at the seafloor. The tentative model presented in Figure 16 must be taken as a preliminary interpretation, and more work, including geochronological studies of magmatic rocks in these complexes is encouraged in order to test this assumption.

7.6.2. Could oceanic structures control the tectono-metamorphic evolution of subducted oceanic crust(s)?

Lithostratigraphic and metamorphic fingerprints in Corsica and in the Western Alps are comparable on many points, and show surprisingly similar prograde P–T patterns (Fig. 15). One can argue that these similarities depend on the fact that the two belts represent part of the same subduction system, thus sharing common setup and metamorphic evolution. However, the two belts probably represent two independent parts of the same orogen, and originated in two distinct, diachronous and

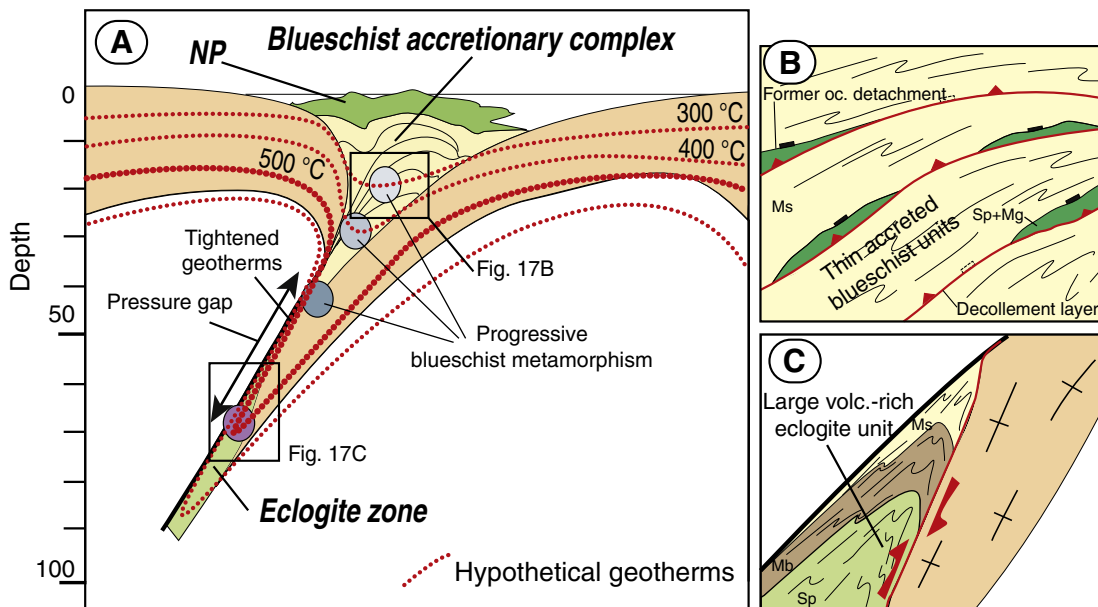


Fig. 17. A) Idealized subduction zone showing the distribution of the BSZ and the EZ with respect to the general trend of geotherms in cold subduction zones. The depth of P–T estimates of the studied samples (circles) based on 0.1 GPa \approx 3.5 km. Note the distribution of the highest-grade circles along a geotherm. B) Close-up of the BSZ accretionary complex. Note the accretion of several slices of metasedimentary rocks, locally floored by ophiolitic basement rocks. This style of accretion is probably favored by the occurrence of talc-rich shear zones in gabbro-rich footwalls of oceanic core complexes (cf. Cannat et al., 2009; Picazo et al., 2012). C) Close-up of the EZ decollement. Note the decollement of a large slice of basalt-rich crust. In this case, the decoupling of the EZ rocks is possibly triggered by the incoming continental margin (cf. discussion in Agard et al., 2009).

possibly opposite subduction zones (cf. discussion in Vitale Brovarone and Herwartz, 2013). Consequently, their similar tectonostratigraphic and metamorphic patterns may be related to a similar mechanical and thermo-mechanical control exerted by inherited oceanic geometries on mountain building.

The interpretation of the metamorphic (blueschist and eclogite) and lithological (metasediment–metabasalt-rich/poor) contrast is twofold. Some authors interpret this contrast to derive from the progressive offscraping of oceanic sedimentary cover rocks at the base of a blueschist-facies accretionary prism, and the subsequent eclogitization of ophiolitic basement rocks at greater depths (Agard et al., 2009; Marthaler and Stampfli, 1989). Other authors refer the lithostratigraphy of the two terranes to two different types of oceanic settings, magma-poor and magma-rich, respectively, also by analogy with present-day settings in slow-spreading oceans (Lagabriele and Cannat, 1990; Tricart and Lagabriele, 1991; Tricart and Lemoine, 1983). Our lithostratigraphic observations likely support the second interpretation. In particular, both zones preserve primary basement-cover sections, but the two types of lithostratigraphic suites are remarkably different, thus indicating two different types of Tethyan lithosphere.

Previous works favoring this paleogeographic signature interpreted the contrasting nature of the two terranes, i.e. metasediment- and metaophiolite-rich, respectively, as the result of two different mechanisms of “decoupling” from the subducting slab of the two basement types (Tricart and Schwartz, 2006). The first domain, lacking thick volcanic layer, exposes mantle rocks or associated gabbros at seafloor by low-angle detachment faults, which are directly covered by oceanic sediments. During subduction, this structure may favor localization of the decollement layer in the upper part of the ophiolitic basement along former oceanic detachment, thus close to the base of the sedimentary pile, and its “shallow” accretion at the base of the prism. The occurrence of a thick network of talc-rich shear zones in gabbro-rich footwalls of present-day settings (Picazo et al., 2012) may represent the key parameter controlling this early and shallower decollement mechanism. Talc-rich layers are also found in the blueschist unit of the studied Alpine belts (e.g. Rocca Bianca zone in the blueschist units of the Western Alps, capped by breccias and pillows) and have been previously considered as Alpine shear zones (Tricart et al., 1982). Our interpretation may imply new considerations on the origin of these features. Hanging walls of these structures in active oceans are less deformed and poor in talc-rich shear zones, and more commonly comprise volcanic rocks. In the EZ of both Corsica and the Western Alps, possible hanging walls of large oceanic extensional structures, ultramafics and sediments are often separated by a thick basaltic layer. This type structure may favor localization of the decollement layer at lower structural levels, possibly at the base of a more intensely serpentinized zone, and the incorporation of thicker ophiolite sequences at greater depth into subduction.

The chronology of metamorphism in the two terranes is similar in Corsica and the Western Alps, with blueschist basalt-poor being subducted prior to basalt-rich domains (cf. review in Agard et al., 2009; Vitale Brovarone and Herwartz, 2013). This feature suggests a slightly earlier subduction of BSZ crust followed by EZ domains. The progressive increase of continental-basement material moving from the “oceanic” BSZ to OCT EZ supports this hypothesis, and suggests the progressive approach of a continental margin to the subduction zone.

The two tectono-metamorphic terranes, i.e. basalt-poor blueschist and basalt-rich eclogite, are systematically juxtaposed in a very precise range of P and T, as revealed by mineral isograds and metamorphic estimates in Alpine Corsica and Western Alps. In particular, their contact statistically corresponds to the T of ca. 470–490 °C and separates rocks that underwent different P (ca. 1.8 GPa versus 2.2–2.4 GPa, Fig. 15). This P–T range may represent a thermomechanic barrier for the two types of basement to be detached from the slab and exhumed. The studied cases indicate that the basalt-rich sequence resists mechanical decoupling until specific metamorphic conditions are reached, i.e.

$T = 470\text{--}490\text{ }^{\circ}\text{C}$ and $P = 2.2\text{--}2.5\text{ GPa}$ (lower limit of the eclogite zone), whereas basalt-poor segments are preferentially detached at blueschist-facies conditions ($T = 330\text{--}470\text{ }^{\circ}\text{C}$, $P = 0.8\text{--}1.8\text{ GPa}$). The key T range of 470–490 °C at which the two terranes juxtapose corresponds to a drastic change in the style of accretion and decollement (Fig. 17). The progressive T increase with the deeper metamorphosed eclogite-facies terranes can be depicted by the topology of the geotherms in the subduction zone, which are tentatively represented in Fig. 17 in an idealized paleotectonic setting for Alpine Corsica. At a depth comparable with the blueschist–eclogite transition in a cold subduction zone, geotherms parallelize to the plate boundary and tighten (cf. e.g. numerical simulations by Hacker, 2003; Syracuse et al., 2010), and T along the plate boundary slightly increases downward. The exhumation and underthrusting of deeper, eclogite-facies material along this interface, possibly triggered by the subduction of a continental margin in the studied cases (see meaning of the Castagniccia unit above), would preserve a rather continuous prograde T_{max} gradient with the shallower blueschist-facies accretionary complex (Fig. 17).

8. Conclusion

The blueschist–eclogite transition in Tethyan belts such as Alpine Corsica or Western Alps is accompanied by contrasting tectonostratigraphic and tectonometamorphic patterns. On one hand, blueschist-facies terranes form by the repeated accretion of volcanic-poor domains of the low-spreading ocean, and show a continuous metamorphic gradient increasing up to 470 °C and 1.8 GPa. On the other hand, eclogite-facies terranes form large and poorly disrupted slices of volcanic-rich slow-spreading oceanic lithosphere. The transition from one to the other occurs at the critical T of ca. 470–490 °C, and is accompanied by a progressive increase of T and by a systematic P gap in the range of 0.6 GPa.

Data discussed in this study suggest that inherited geometries, such as multiple detachment generations and oceanic core complexes in slow-spreading oceans may have a crucial role in the mechanism of accretion or subduction and mountain building. Field observations and comparisons with active analogs in present-day oceans show that these structures have different lithological associations and structures that may exert a precise mineralogical/mechanical control on selective exhumation of blueschist- and eclogite-facies material in orogenic belts.

Acknowledgments

The authors thank Alexis Plunder, Philippe Agard, Roberto Compagnoni and Jacques Malavieille for fruitful discussions. Mathilde Cannat is also deeply thanked for discussion on OCC. MP and AVB thank T. Quilici and the Casanova family for their hospitality during fieldwork. John Wakabayashi and an anonymous reviewer are thanked for their comments and suggestions that greatly improved the manuscript, and Laurent Jolivet for editorial handling. This work was supported by French state funds managed by the ANR within the Investissements d’Avenir programme under reference ANR-11-IDEX-0004-02, and more specifically within the framework of the Cluster of Excellence MATISSE. Research funding by CNRS INSU (programme Syster) is acknowledged.

References

- Agard, P., Yamato, P., Jolivet, L., Burov, E., 2009. Exhumation of oceanic blueschists and eclogites in subduction zones: timing and mechanisms. *Earth-Sci. Rev.* <http://dx.doi.org/10.1016/j.earscirev.2008.11.002>.
- Amaudric du Chaffaut, S., 1972. Données nouvelles sur la stratigraphie des Schistes Lustrés de Corse: la série de l’Inzecca. Comparaisons avec les Alpes Occidentales et l’Apennin ligurien. *C. R. Acad. Sci. Paris* 275, 2611–2614.
- Angiboust, S., Agard, P., Jolivet, L., Beyssac, O., 2009. The Zermatt-Saas ophiolite: the largest (60-km wide) and deepest (c.70–80 km) continuous slice of oceanic lithosphere detached from a subduction zone? *Terra Nova* 21, 171–180.

- Angiboust, S., Langdon, R., Agard, P., Waters, D., Chopin, C., 2011. Eclogitization of the Monviso ophiolite (W. Alps) and implications on subduction dynamics. *J. Metamorph. Geol.* 30, 37–61.
- Ballèvre, M., Lagabrielle, Y., 1994. Garnet in blueschist-facies marbles from the Queyras unit (Western Alps): its occurrence and its significance. *Schweiz. Mineral. Petrogr. Mitt.* 74, 193–201.
- Ballèvre, M., Merle, R., 1990. Tertiary ductile normal faulting as a consequence of lithospheric stacking in the Western Alps. *Soc. Géol. Fr. Mém.* 156, 227–236.
- Ballèvre, M., Merle, R., 1993. The Combin Fault: compressional reactivation of a Late Cretaceous–Early Tertiary detachment fault in the Western Alps. *Schweiz. Mineral. Petrogr. Mitt.* 73, 205–227.
- Beltrando, M., Rubatto, D., Manatschal, G., 2010a. From passive margins to orogens: the link between ocean–continent transition zones and (ultra)high-pressure metamorphism. *Geology* 38, 559–562.
- Beltrando, M., Compagnoni, R., Lombardo, B., 2010b. (Ultra-) High-pressure metamorphism and orogenesis: An Alpine perspective. *Gondwana Research* 18, 147–166. <http://dx.doi.org/10.1016/j.gr.2010.01.009>.
- Beltrando, M., Manatschal, G., Mohn, G., Dal Piaz, G.V., Vitale Brovarone, A., Masini, E., 2014. Recognizing remnants of magma-poor rifted margins in high-pressure orogenic belts: The alpine case study. *Earth Science Reviews* (in press).
- Beysac, O., Goffé, B., Chopin, C., Rouzaud, J.-N., 2002. Raman Spectra of Carbonaceous Material in Metasediments: A New Geothermometer. *Earth Planet. Sci. Lett.* 225, 233–241.
- Beysac, O., Brunet, F., Petitet, J.-P., Goffé, B., Rouzaud, J.-N., 2003. Experimental study of the microtextural and structural transformations of carbonaceous materials under pressure and temperature. *Eur. J. Mineral.* 15, 937–951.
- Beysac, O., Bollinger, L., Avouac, J.P., Goffé, B., 2004. Thermal metamorphism in the lesser Himalaya of Nepal determined from Raman spectroscopy of carbonaceous material. *Earth Planet. Sci. Lett.* 225, 233–241.
- Blanco-Quintero, I.F., Garcia-Casco, A., Gerya, T.V., 2010. Tectonic blocks in serpentinite melange (eastern Cuba) reveal large-scale convective flow of the subduction channel. *Geology* 39, 79–82.
- Brown, M., 2007. Metamorphic conditions in orogenic belts: a record of secular change. *Int. Geol. Rev.* 49, 193–234.
- Caby, R., 1995. Plastic Deformation of Gabbros in a Slowspreading Mesozoic Ridge: Example of the Mongen\evre Ophiolite, Western Alps. In: Vissers, R.L.M., Nicolas, A. (Eds.), *Mantle and Lower Crust Exposed in Oceanic Ridges and in Ophiolites*. Kluwer Academic Publishers, pp. 123–145.
- Caby, R., Michard, A., Tricart, P., 1971. Découverte d'une brèche polygénique à éléments granitoides dans les ophiolites métamorphiques piémontaises (Schistes lustrés du Queyras, Alpes françaises). *C. R. Acad. Sci. IIA – Earth Planet. Sci.* 273, 999–1002.
- Cannat, M., Sauter, D., Escartín, J., Lavier, L., Picazo, S., 2009. Earth and planetary science letters. *Earth Planet. Sci. Lett.* 288, 174–183.
- Caron, J.M., Delcey, R., 1979. Lithostratigraphie des schistes lustrés corses: diversité des séries post-ophiolitiques. *C. R. Acad. Sci.* 208, 1525–1528.
- Castelli, D., Rollo, F., Groppo, C., Compagnoni, R., 2007. Impure marbles from the UHP Brossasco–Isasca Unit (Dora–Maira Massif, Western Alps): evidence for Alpine equilibration in the diamond stability field and evaluation of the X(CO₂) fluid evolution. *Geology* 35, 587–603.
- Cloos, M., 1993. Lithospheric buoyancy and collisional orogenesis: subduction of oceanic plateaus, continental margins, island arcs, spreading ridges, and seamounts. *Geol. Soc. Am. Bull.* 105, 715.
- Cloos, M., Shreve, R.L., 1988. Subduction–channel model of prism accretion, melange formation, sediment subduction, and subduction erosion at convergent plate margins: 2. Implications and discussion. *Pure Appl. Geophys.* 128, 501–545.
- Connolly, J.A.D., 2009. The geodynamic equation of state: what and how. *Geochim. Geophys. Geosyst.* 10, Q10014.
- Deville, E., Fudral, S., Lagabrielle, Y., Marthaler, M., Sartori, M., 1992. From oceanic closure to continental collision: a synthesis of the “Schistes lustrés” metamorphic complex of the Western Alps. *Geol. Soc. Am. Bull.* 104, 127–139.
- Durand-Delga, M., 1978. Corse. Guides géologiques régionaux. Masson, Pa.ed.
- Ernst, W.G., Maruyama, S., Wallis, S., 1997. Buoyancy-driven, rapid exhumation of ultrahigh-pressure metamorphosed continental crust. *Proc. Natl. Acad. Sci. U. S. A.* 94, 9532–9537.
- Gabalda, S., Beyssac, O., Jolivet, L., Agard, P., Chopin, C., 2009. Thermal structure of a fossil subduction wedge in the Western Alps. *Terra Nova* 21, 28–34.
- Ghent, E.D., Tinkham, D., Marr, R., 2009. Lawsonite eclogites from the Pinchi Lake area, British Columbia – new P–T estimates and interpretation. *Lithos* 109, 248–253.
- Goto, A., Kunugiza, K., Omori, S., 2007. Evolving fluid composition during prograde metamorphism in subduction zones: a new approach using carbonate-bearing assemblages in the pelitic system. *Gondwana Res.* 11, 166–179.
- Groppo, C., Castelli, D., 2010. Prograde P–T evolution of a lawsonite eclogite from the Monviso meta-ophiolite (Western Alps): dehydration and redox reactions during subduction of oceanic FeTi-oxide gabbro. *J. Petrol.* 51, 2489–2514.
- Guillot, S., Hattori, K., Agard, P., Schwartz, S., Vidal, O., 2009. Exhumation Processes in Oceanic and Continental Subduction Contexts: A Review. Springer, Berlin, Heidelberg.
- Hacker, B.R., 2003. Subduction factory 1. Theoretical mineralogy, densities, seismic wave speeds, and H₂O contents. *J. Geophys. Res.* 108, 2029.
- Holland, T.J.B., Powell, R., 1996. Thermodynamics of order–disorder in minerals. 2. Symmetric formalism applied to solid solutions. *American Mineralogist* 81, 1425–1437.
- Holland, T.J.B., Powell, R., 1998. An internally consistent thermodynamic data set for phases of petrologic interest. *Journal of Metamorphic Geology* 16, 309–343.
- Jolivet, L., Dubois, R., Fournier, M., Goffé, B., Michard, A., Jourdan, C., 1990. Ductile extension in Alpine Corsica. *Geology* 18, 1007–1010.
- Klein, F., Garrido, C.J., 2011. Thermodynamic constraints on mineral carbonation of serpentinitized peridotite. *Lithos* 126, 147–160.
- Lagabrielle, Y., 1987. Les ophiolites: Marqueurs de l'histoire tectonique des domaines océaniques. (Thesis) Univ. Brest, France (350 pp.).
- Lagabrielle, Y., 1994. Ophiolites of the Western Alps and the nature of the Tethyan oceanic lithosphere. *Ophioliti* 19, 413–434.
- Lagabrielle, Y., 2009. Mantle exhumation and lithospheric spreading: an historical perspective from investigations in the oceans and in the Alps–Apennines ophiolites. *Boll. Soc. Geol. Ital.* 1–30.
- Lagabrielle, Y., Cannat, M., 1990. Alpine Jurassic ophiolites resemble the modern central Atlantic basement. *Geology* 18, 319–322.
- Lagabrielle, Y., Lemoine, M., 1997. Alpine, Corsican and Apennine ophiolites: the slow-spreading ridge model. *C. R. Acad. Sci.* 325, 909–920.
- Lagabrielle, Y., Polino, R., 1985. Origine volcano-détritique de certaines prasinites des Schistes lustrés du Queyras (France): arguments texturaux et géochimiques. *Bull. Soc. Geol. Fr.* 4, 461–471.
- Lahfid, A., Beyssac, O., Deville, E., Negro, F., Chopin, C., Goffé, B., 2010. Evolution of the Raman spectrum of carbonaceous material in low-grade metasediments of the Glarus Alps (Switzerland). *Terra Nova* 22, 354–360.
- Lahondère, D., 1996. Les schistes bleus et les éclogites à lawsonite des unités continentales et océaniques de la Corse alpine: nouvelles données pétrologiques et structurales (Corse). BRGM. ed.
- Lahondère, D., Rossi, P., Lahondère, J.C., 1999. Structuration alpine d'une marge continentale externe: le massif du Tenda (Haute-Corse). Implications géodynamiques au niveau de la transversale Corse–Apennins. *Géol. Fr.* 4, 27–44.
- Lavier, L., Manatschal, G., 2006. A mechanism to thin the continental lithosphere at magma-poor margins. *Nature* 440, 324–328.
- Le Mer, O., Lagabrielle, Y., Polino, R., 1986. Une série sédimentaire détritico liée aux ophiolites piémontaises: analyses lithostratigraphiques, texturales et géochimiques dans le massif de la Crete Mouloun (Haut Queyras, Alpes sud-occidentales, France). *Géol. Alpine* 62, 63–86.
- Lemoine, M., 1980. Serpentinites, gabbros and ophiocarbonates in the Piedmont–Ligurian domain of the Western Alps, possible indicators of oceanic fracture zones and associated serpentinite protrusions in the Jurassic–Cretaceous Tethys. *Arch. Sci. Genève* 33, 103–116.
- Lemoine, M., 2003. Schistes lustrés from Corsica to Hungary: back to the original sediments and tentative dating of partly azoic metasediments. *Bull. Soc. Geol. Fr.* 174, 197–209.
- Lemoine, M., Boillot, P., Tricart, G., 1987. Ultramafic and gabbroic ocean floor of the Ligurian Tethys (Alps, Corsica, Apennines). In search of a genetic model. *Geology* 15, 622–625.
- Levi, N., Malasoma, A., Marroni, M., Pandolfi, L., Paperini, M., 2007. Tectono-metamorphic history of the ophiolitic Lento unit (Northern Corsica): evidences for the complexity of accretion–exhumation processes in a fossil subduction system. *Geodin. Acta* 20, 99–118.
- Lombardo, B., Nervo, R., Compagnoni, R., Messiga, B., Kienast, J., Mevel, C., Fiora, L., Piccardo, G.B., 1978. Osservazioni preliminari sulle ophioliti metamorfiche del Monviso (Alpi occidentali). *Rend. Soc. Ital. Mineral. Petrol.* 34, 253–305.
- Lombardo, B., Rubatto, D., Castelli, D., 2002. Ion microprobe U–Pb dating of zircon from a Monviso metaplagiogrante: implications for the evolution of the Piedmont–Liguria Tethys in the Western Alps. *Ophioliti* 27, 109–117.
- Malatesta, C., Crispini, L., Federico, L., Capponi, G., Scambelluri, M., 2011. Tectonophysics. *Tectonophysics* 1–22.
- Malavieille, J., Chemenda, A., Larroque, C., 1998. Evolutionary model for Alpine Corsica: mechanism for ophiolite emplacement and exhumation of high-pressure rocks. *Terra Nova* 10, 317–322. <http://dx.doi.org/10.1046/j.1365-3121.1998.00208.x>.
- Manatschal, G., Müntener, O., 2009. Tectonophysics. *Tectonophysics* 473, 4–19.
- Mancktelow, N., 2008. Tectonic overpressure: theoretical concepts and modelled examples. *Lithos* 103, 149–177.
- Marthaler, M., Stampfli, G.M., 1989. Les Schistes lustrés à ophiolites de la nappe du Tsaté: un ancien prisme d'accrétion de la marge active apulienne? *Schweiz. Mineral. Petrogr. Mitt.* 69, 211–216.
- Martin, L., Rubatto, D., Vitale Brovarone, A., Hermann, J., 2011. Late Eocene lawsonite–eclogite facies metasomatism of a granulite sliver associated to ophiolites in Alpine Corsica. *Lithos* 125, 620–640.
- Maruyama, S., Liou, J.G., Terabayashi, M., 1996. Blueschists and eclogites of the world and their exhumation. *Int. Geol. Rev.* 38, 485–594.
- Mattauer, M., Faure, M., Malavieille, J., 1981. Transverse lineation and large-scale structures related to Alpine obduction in Corsica. *J. Struct. Geol.* 3, 401–409.
- Meresse, F., Lagabrielle, Y., Malavieille, J., Ildefonse, B., 2012. A fossil Ocean–Continent Transition of the Mesozoic Tethys preserved in the Schistes lustrés nappe of northern Corsica. *Tectonophysics* 579, 4–16.
- Molli, G., 2008. Northern Apennine–Corsica orogenic system: an updated overview. *Geol. Soc. Lond. Spec. Publ.* 298, 413–442.
- Molli, G., Tribuzio, R., Marquer, D., 2006. Deformation and metamorphism at the eastern border of the Tenda Massif (NE Corsica): a record of subduction and exhumation of continental crust. *J. Struct. Geol.* 28, 1748–1766.
- Newton, R.C., Charlu, T.V., Kleppa, O.J., 1980. Thermochemistry of the high structural state plagioclases. *Geochimica et Cosmochimica Acta* 44, 933–941.
- Ota, T., Kaneko, Y., 2010. Gondwana research. *Gondwana Res.* 18, 167–188.
- Péquignot, G., Potdevin, J., 1984. Métamorphisme et tectonique dans les Schistes lustrés à l'Est de Corte (Corse). Univ. Claude-Bernard (Lyon).
- Picazo, S., Manatschal, G., Cannat, M., 2011. Exhumed mantle along an Ocean Continent Transition: the example of the Totalp ophiolite in SE Switzerland. Presented at the EGU General Assembly, Vienna, Austria.
- Picazo, S., Cannat, M., Delacour, A., Escartín, J., Rouméjon, S., Silantsev, S., 2012. Deformation associated with the denudation of mantle-derived rocks at the Mid-Atlantic Ridge 13°–15°N: the role of magmatic injections and hydrothermal alteration. *Geochim. Geophys. Geosyst.* 13 (n/a–n/a).

- Plunder, A., Agard, P., Dubacq, B., Chopin, C., Bellanger, M., 2012. How continuous and precise is the record of P–T paths? Insights from combined thermobarometry and thermodynamic modelling into subduction dynamics (Schistes Lustrés, W. Alps). *30*, 323–346.
- Polino, R., Lemoine, M., 1984. Détritisme mixte d'origine continentale et océanique dans les sédiments jurassico-crétacés supra-ophiolitiques de la Téthys Ligure: la série du Lago Nero (Alpes Occidentales franco-italiennes). *C. R. Acad. Sci.* 298, 359–364.
- Principi, G., Treves, B., 1984. Il sistema corso-appenninico come prisma d'accreszione. Riflessi sul problema generale del limite Alpi-Appennini. *Mem. Soc. Geol. Ital.* 28, 549–576.
- Puccinelli, A., Perilli, N., Cascella, A., 2012. Stratigraphy of the Caporalino–Sant'Angelo unit: a fake Jurassic–Eocene succession of the 'Alpine' Corsica. *Riv. Ital. Paleontol. Stratigr.* 118, 471–491.
- Ravna, E.J.K., Andersen, T.B., Jolivet, L., de Capitani, C., 2010. Cold subduction and the formation of lawsonite eclogite – constraints from prograde evolution of eclogitized pillow lava from Corsica. *J. Metamorph. Geol.* 28, 381–395.
- Rossi, P., Durand-Delga, M., Caron, J.M., Guieu, G., Conchon, O., Libourel, G., Loÿe-Pilot, M.-D., 1994. Notice explicative, Carte géologique de France (1/50,000), feuille Corte (1110). BRGM (No. 224), Orléans.
- Rossi, P., Durand-Delga, M., COLL, A., 2002. Carte géol. France (1/50,000), feuille Santo Pietro di Tenda (1106). BRGM, Orléans.
- Sauter, D., Cannat, M., Rouméjon, S., Andreani, M., Birot, D., Bronner, A., Brunelli, D., Carlot, J., Delacour, A., Guyader, V., MacLeod, C.J., Manatschal, G., Mendel, V., Ménez, B., Pasini, V., Ruellan, E., Searle, R., 2013. Continuous exhumation of mantle-derived rocks at the Southwest Indian Ridge for 11 million years. *Nat. Geosci.* 6, 314–320.
- Schwartz, S., Guillot, S., Reynard, B., Lafay, R., Nicollet, C., Debret, B., Lanari, P., Auzende, A.L., 2012. Pressure–temperature estimates of the lizardite/antigorite transition in high pressure serpentinites. *Lithos* 197–210.
- Smith, D.K., Escartin, J., Schouten, H., Cann, J.R., 2008. Fault rotation and core complex formation: significant processes in seafloor formation at slow-spreading mid-ocean ridges (Mid-Atlantic Ridge, 13–15 N). *Geochem. Geophys. Geosyst.* 9.
- Syracuse, E.M., van keken, P.E., Abers, G.A., 2010. The global range of subduction zone thermal models. *Phys. Earth Planet. Inter.* 183, 73–90.
- Tricart, P., 1974. Les Schistes lustrés du Haut-Cristillan (Alpes cottiennes, France): lithostratigraphie, architecture et tectonogénese. *Géol. Alpine* 50, 131–152.
- Tricart, P., Lagabrielle, Y., 1991. The Queyras ophiolite west of Monte Viso (Western Alps): indicator of a peculiar ocean floor in the Mesozoic Tethys. *J. Geodyn.* 13, 163–181.
- Tricart, P., Lemoine, M., 1983. No serpentinite oceanic bottom in South Queyras ophiolites (French Western Alps): record of the incipient oceanic opening of the Mesozoic Ligurian Tethys. *Eclogae Geol. Helv.* 76, 611–629.
- Tricart, P., Schwartz, S., 2006. A north–south section across the Queyras Schistes lustrés (Piedmont zone, Western Alps): syn-collision refolding of a subduction wedge. *Eclogae Geol. Helv.* 99, 429–442.
- Tricart, P., Bourbon, M., Lagabrielle, Y., 1982. Révision de la coupe Péouvou-Roche Noire (zone piémontaise, Alpes franco-italiennes): bréchification synsédimentaire d'un fond océanique ultrabasique. *Géol. Alpine* 58, 105–113.
- Tsujiyori, T., Sisson, V.B., Liou, J.G., Harlow, G.E., Sorensen, S.S., 2006. Very-low-temperature record of the subduction process: a review of worldwide lawsonite eclogites. *Lithos* 92, 609–624.
- Vitale Brovarone, 2013. Lawsonite-bearing omphacitites from Alpine Corsica (France). *Int. J. Earth Sci.* 102, 1377–1379.
- Vitale Brovarone, A., Agard, P., 2013. True metamorphic isograds or tectonically sliced metamorphic sequence? New high-spatial resolution petrological data for the New Caledonia case study. *Contrib. Mineral. Petrol.* 166, 451–469.
- Vitale Brovarone, A., Herwartz, D., 2013. Timing of HP metamorphism in the Schistes Lustrés of Alpine Corsica: new Lu–Hf garnet and lawsonite ages. *Lithos* 172–173, 175–191.
- Vitale Brovarone, A., Groppo, C., Hetényi, G., Compagnoni, R., Malavieille, J., 2011a. Coexistence of lawsonite-bearing eclogite and blueschist: phase equilibria modelling of Alpine Corsica metabasalts and petrological evolution of subducting slabs. *J. Metamorph. Geol.* 29, 583–600.
- Vitale Brovarone, A., Beltrando, M., Malavieille, J., Giuntoli, F., Tondella, E., Groppo, C., Beyssac, O., Compagnoni, R., 2011b. Inherited Ocean–Continent Transition zones in deeply subducted terranes: insights from Alpine Corsica. *Lithos* 124, 273–290.
- Vitale Brovarone, A., Beyssac, O., Malavieille, J., Molli, G., Beltrando, M., Compagnoni, R., 2013. Stacking and metamorphism of continuous segments of subducted lithosphere in a high-pressure wedge: the example of Alpine Corsica (France). *Earth-Sci. Rev.* 116, 35–56.
- Vitale Brovarone, A., Beyssac, O., Alard, O., Martin, L., Picatto, M., 2014. Lawsonite metasomatism and trace element recycling in subduction zones. *Journal of Metamorphic Geology* (in press).
- Wakabayashi, J., 2012. Subducted sedimentary serpentinite mélanges: record of multiple burial–exhumation cycles and subduction erosion. *Tectonophysics* 568–569, 230–247.
- Wei, C.J., Powell, R., 2003. Phase relations in high-pressure metapelites in the system KFMASH (K_2O – FeO – MgO – Al_2O_3 – SiO_2 – H_2O) with application to natural rocks. *Contributions to Mineralogy and Petrology* 145, 301–315.
- White, R.W., Powell, R., Holland, T.J.B., Worley, B.A., 2000. The effect of TiO_2 and Fe_2O_3 on metapelitic assemblages at greenschist and amphibolite facies conditions: mineral equilibria calculations in the system K_2O – FeO – MgO – Al_2O_3 – SiO_2 – H_2O – TiO_2 – Fe_2O_3 . *Journal of Metamorphic Geology* 18, 497–511.
- White, R.W., Powell, R., Phillips, G.N., 2003. A mineral equilibria study of the hydrothermal alteration in mafic greenschist facies rocks at Kalgoolie, Western Australia. *Journal of Metamorphic Geology* 21, 455–468.